HDL-TM-80-31

November 1980

Performance of Ram Air Driven Power Supply for Proposed High Altitude Rocket in Naval Surface Weapons Center Supersonic Wind Tunnel

By Jonathan E. Fine

U.S. Army Electronics Research and Development Command

Harry Diamond Laboratories

Adelphi, MD 20783

The findings in this report are not to be construed as an official Department of the Army position unless so designated by other authorized documents.

Citation of manufacturers' or trade names does not constitute an official indorsement or approval of the use thereof.

Destroy this report when it is no longer needed. Do not return it to the originator.

UNCLASSIFIED

SECURITY CLASSIFICATION OF THIS PAGE *(When Date Entered)*

REPORT DOCUMENTATION PAGE		READ INSTRUCTIONS BEFORE COMPLETING FORM
1. REPORT NUMBER HDL-TM-80-31	2. GOVT ACCESSION NO.	3. RECIPIENT'S CATALOG NUMBER
4. TITLE *(and Subtitle)* Performance of Ram Air Driven Power Supply for Proposed High Altitude Rocket in Naval Surface Weapons Center Supersonic Wind Tunnel		5. TYPE OF REPORT & PERIOD COVERED Technical Memorandum 6. PERFORMING ORG. REPORT NUMBER
7. AUTHOR(s) by Jonathan E. Fine		8. CONTRACT OR GRANT NUMBER(s)
9. PERFORMING ORGANIZATION NAME AND ADDRESS Harry Diamond Laboratories 2800 Powder Mill Road Adelphi, MD 20783		10. PROGRAM ELEMENT, PROJECT, TASK AREA & WORK UNIT NUMBERS Program Ele: 6.33.03.A
11. CONTROLLING OFFICE NAME AND ADDRESS PM/Multiple Launch Rocket System Naval Service Weapons Center, White Oak Silver Spring MD 20910		12. REPORT DATE November 1980 13. NUMBER OF PAGES 47
14. MONITORING AGENCY NAME & ADDRESS *(if different from Controlling Office)*		15. SECURITY CLASS. *(of this report)* Unclassified 15a. DECLASSIFICATION/DOWNGRADING SCHEDULE

16. DISTRIBUTION STATEMENT *(of this Report)*

Approved for public release; distribution unlimited.

17. DISTRIBUTION STATEMENT *(of the abstract entered in Block 20, if different from Report)*

18. SUPPLEMENTARY NOTES

HDL Project: 4249D6
DRCMS Code: 6433035640012
DA Project: 1X463303D564

19. KEY WORDS *(Continue on reverse side if necessary and identify by block number)*

Air-driven generator	Environmental signature	Trajectory performance simulation
Fluidic generator	Safety and arming	Wind energy for fuze
Battery	Rocket fuze	Multiple Launch Rocket System (MLRS)
Power supply	Simulation of fuze performance	

20. ABSTRACT *(Continue on reverse side if necessary and identify by block number)*

A ram air driven power supply for the Multiple Launch Rocket System (MLRS) air vehicle was tested with a fuze in the Naval Surface Weapons Center Supersonic Wind Tunnel Facility. The power supply operated the fuze over the apex of a probable flight trajectory where the generator's inlet ram air energy input is small. A method has been devised to relate laboratory, wind tunnel, and field test data so that expected voltages in flight or in the wind tunnel can be obtained from laboratory measurements.

DD FORM 1 JAN 73 1473 EDITION OF 1 NOV 65 IS OBSOLETE

UNCLASSIFIED

SECURITY CLASSIFICATION OF THIS PAGE *(When Date Entered)*

CONTENTS

FIGURES

FIGURES (Cont'd)

TABLES

Page

1. INTRODUCTION

Tests were conducted at the Naval Surface Weapons Center (NSWC), White Oak Laboratories, Supersonic Wind Tunnel Facility on 7, 8, and 11 September 1978 to determine the ability of the ram air driven power supply to power the fuze during the high altitude portions of the trajectory of the Multiple Launch Rocket System (MLRS) air vehicle.

These tests are similar to those conducted in November 1977 at NSWC,[1] except that the fluidic generator has been improved to produce a higher voltage near the apex, and the electrical load is the fuze rather than a resistance and a capacitance.

A drawing of the fluidic generator power supply mounted in a fuze ogive is shown in figure 1. During flight, air enters the generator through the single entrance port in the nose and leaves through exhaust ports uniformly spaced around the circumference of the ogive. During the passage through the generator, the air vibrates a resonant chamber that transmits its oscillations through a mechanical diaphragm and rod to a reed that switches magnetic flux within a coil, thereby inducing a voltage at the coil terminals.

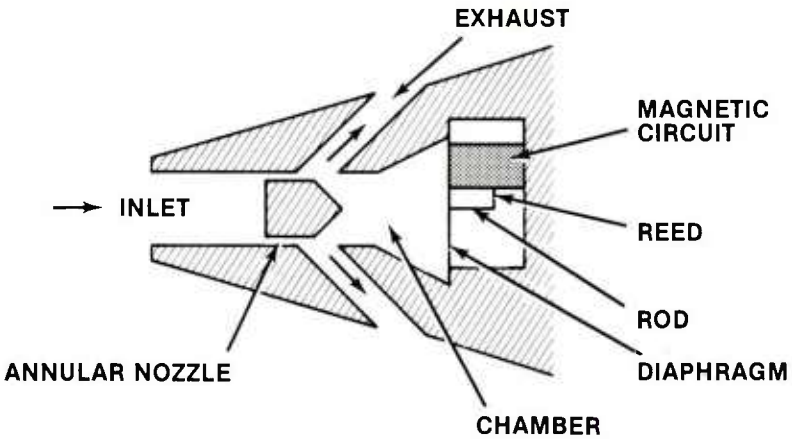

Figure 1. Air passage through ogive containing fluidic generator power supply.

The coil terminals are connected to the fuze, which is mounted as shown in figure 2, on the wind tunnel sting. Leads from three selected locations in the fuze electronic circuit are brought out of the wind tunnel by a long shielded multiconductor cable. The fuze circuit contains a full wave bridge, across which the generator terminals are connected (fig. 3). The signal across one leg of the bridge is reduced by a voltage divider. The reduced signal is the power supply monitor signal and is obtained on one of the leads brought out from the fuze. The monitor signal voltage has the same frequency as the generator and can be calibrated in terms of voltage at the fuze input terminals. The second lead is brought out from a scaler circuit within the fuze. The scaler signal is a constant amplitude 10-Hz square wave that begins when the voltage input to the fuze reaches a value of 55 V peak to peak (p-p). Presence of the scaler signal indicates that the fuze is

[1] *Jonathan E. Fine, Analysis of Wind Tunnel Test Results of Fluidic Generator for High-Altitude Rocket, Harry Diamond Laboratories HDL-TR-1877 (March 1979).*

operational. The third lead is brought out from the fuze circuit ground. By observing the monitor and the scaler signals, the input voltage and the frequency to the fuze from the power supply can be determined and related to the operating condition of the fuze.

The laboratory calibration procedure enabled the fuze operation to be determined in terms of parameters that can be measured in the wind tunnel.

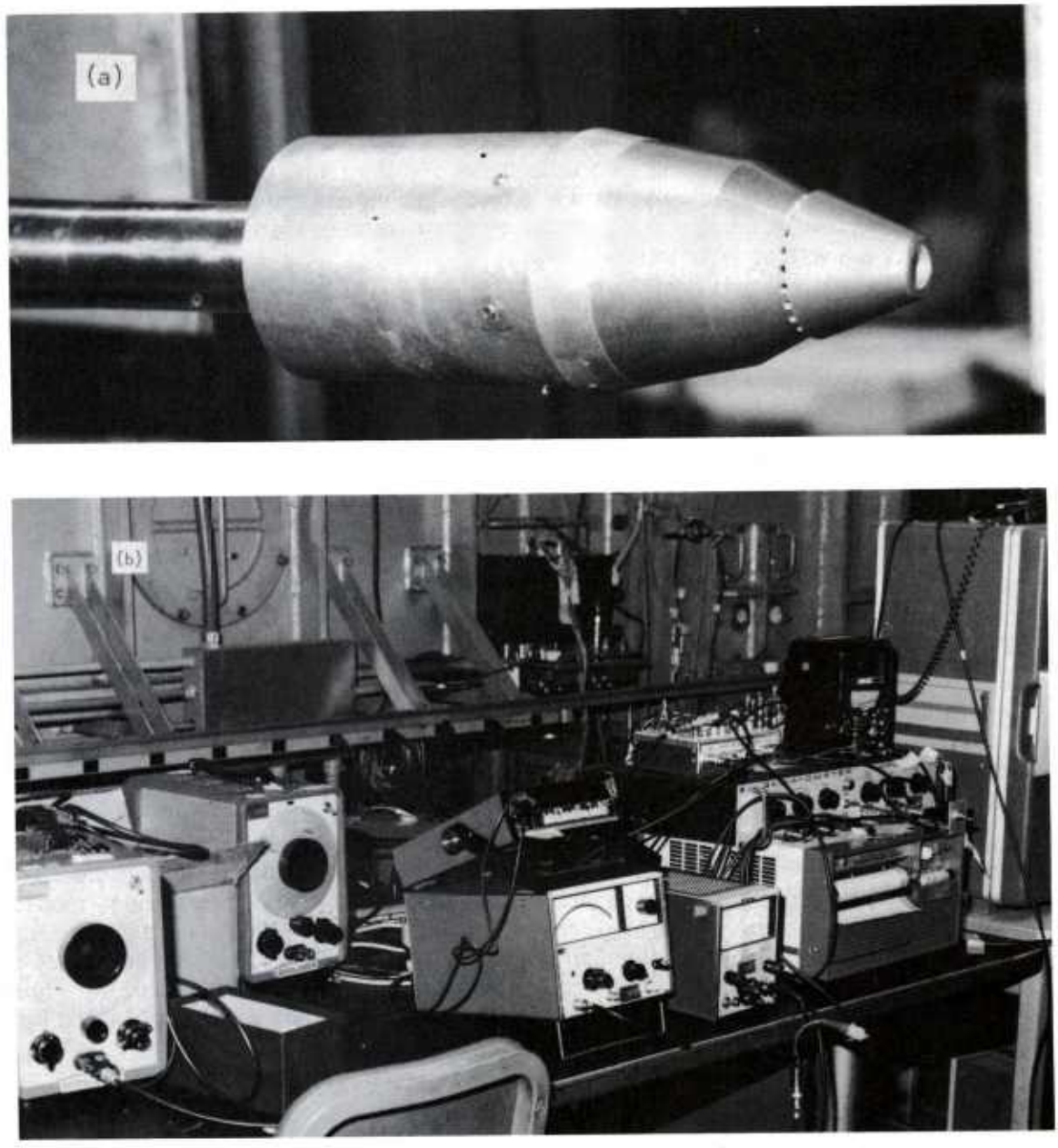

Figure 2. Wind tunnel test setup: (a) fuze mounted in wind tunnel sting and (b) instrumentation.

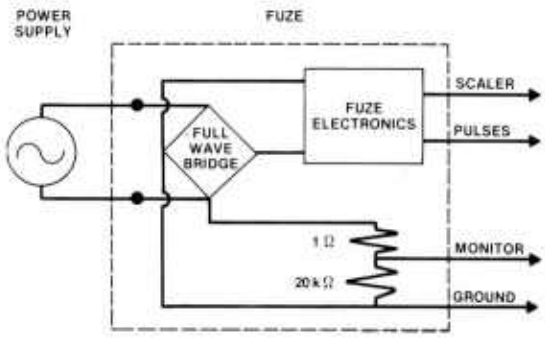

Figure 3. Diagram of fuze circuit showing connections to power supply and instrumentation.

2. LABORATORY CALIBRATION

The laboratory calibration included two tests. Because the fuze had no extra connections to the input terminals, the fuze input could not be monitored directly during the wind tunnel test. Hence, the first test was to use a signal generator having an adjustable amplitude and an impedance matching transformer to apply voltage signals of various levels to the fuze input and observe the monitor and scaler signals from each terminal. The calibration curve of monitor voltage (volts root mean square—rms) versus fuze input voltage is shown in figure 4. For this fuze, the scaler comes on at 55 Vp-p. With this curve, the input voltage values can be read from the monitor signal amplitudes obtained during the wind tunnel test.

A second calibration test was performed to relate the observed fuze signals to laboratory conditions of pressure that could be related to wind tunnel conditions. A diagram of the apparatus and the instrumentation is shown in figure 5.

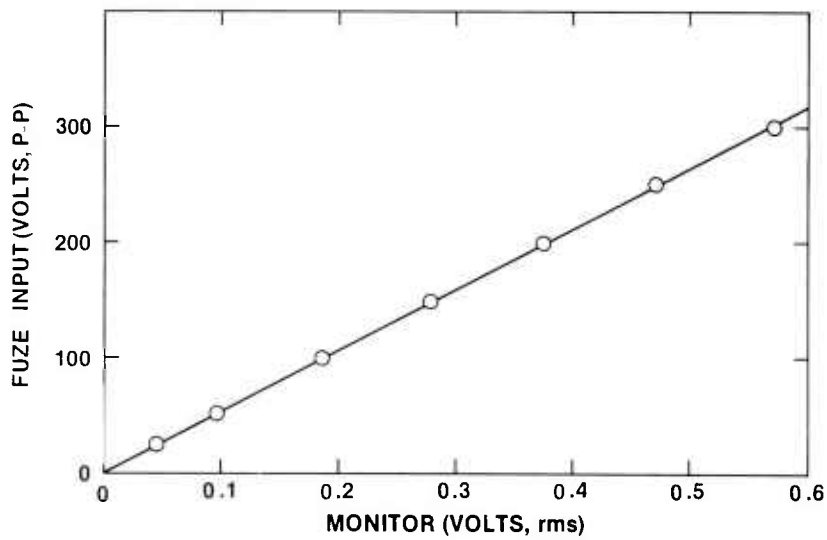

Figure 4. Calibration curve for fuze input voltage in terms of monitor voltage.

Figure 6 shows the fuze input voltage versus the supply pressure for the fluidic generator. These values of supply pressure cover the range of voltage values expected in the wind tunnel test.

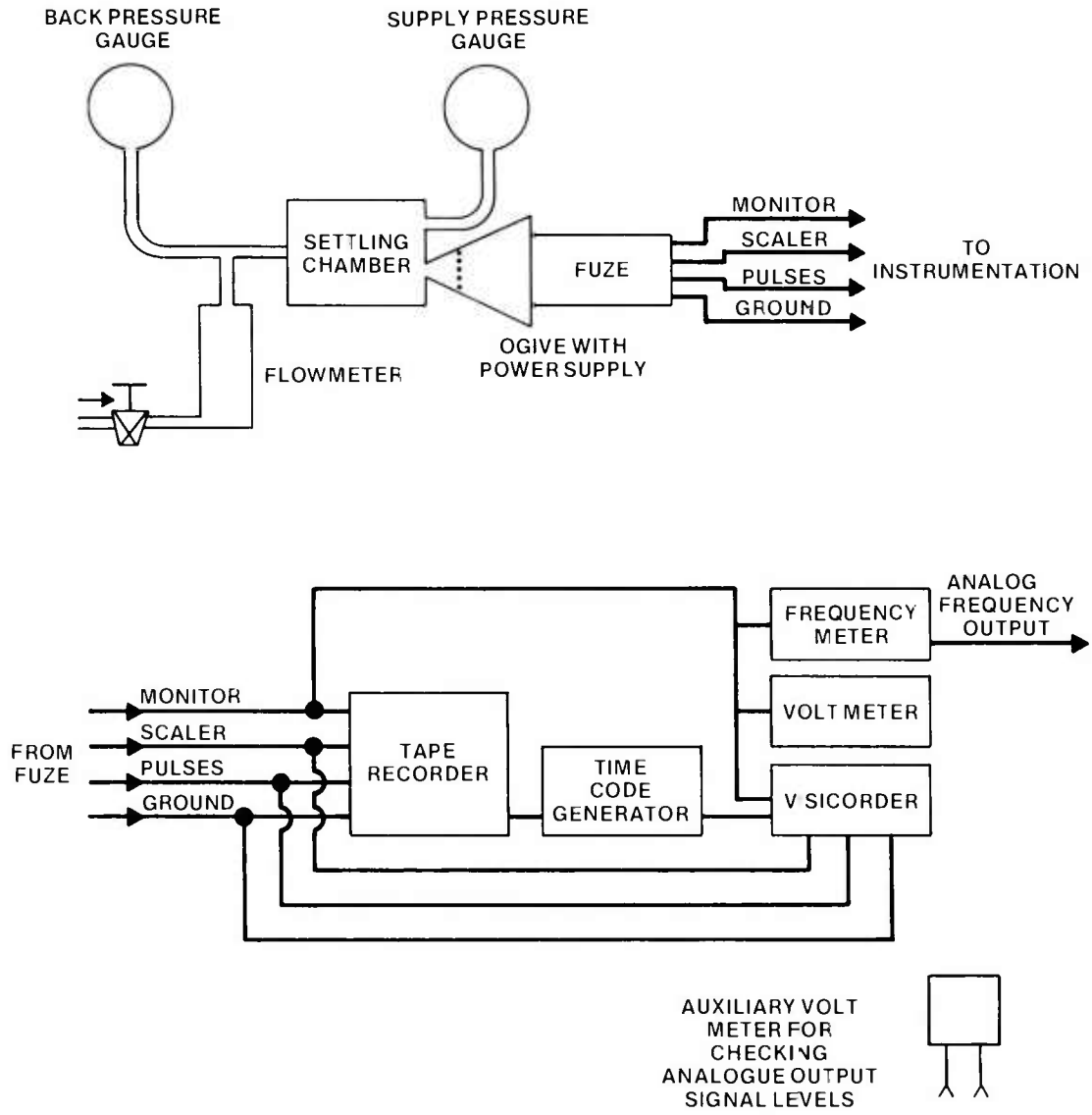

Figure 5. Diagram of laboratory instrumentation.

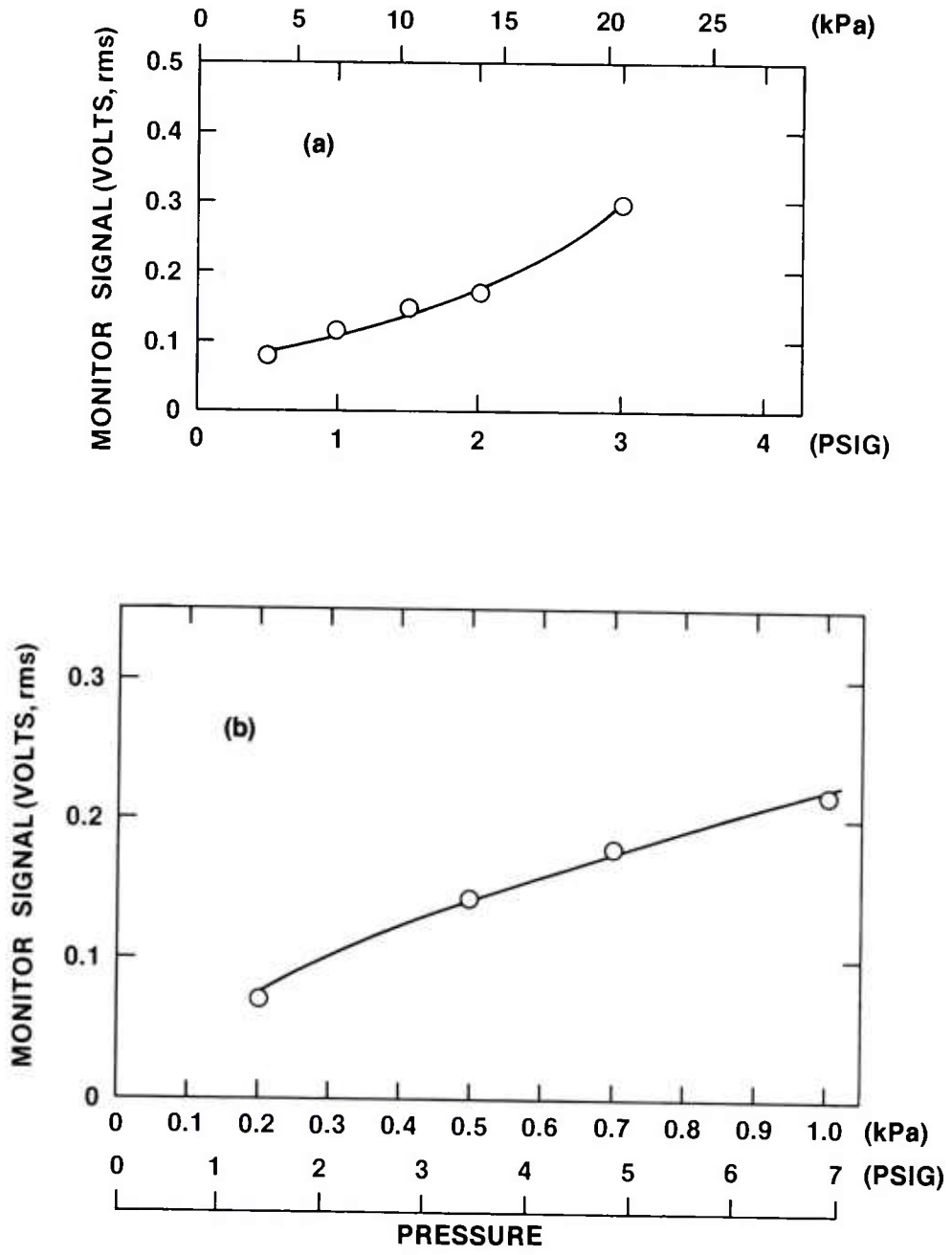

Figure 6. Laboratory data of monitor voltage versus supply pressure: (a) for fluidic generator 40 and (b) for alternator H-536.

3. PROCEDURE FOR WIND TUNNEL TEST

A diagram of the instrumentation used in the wind tunnel test is shown in figure 7. The generator monitor signal and the scaler signals are recorded on the visicorder and on magnetic tape along with the wind tunnel parameters of total pressure (p_o) and total temperature (T_o). The following procedure was followed in the wind tunnel. The total pressure was brought up to a value that was maintained until the occurrence of supersonic flow was verified by visual inspection of the flow pattern. Monitor and scaler voltages were then recorded for the values of tunnel total

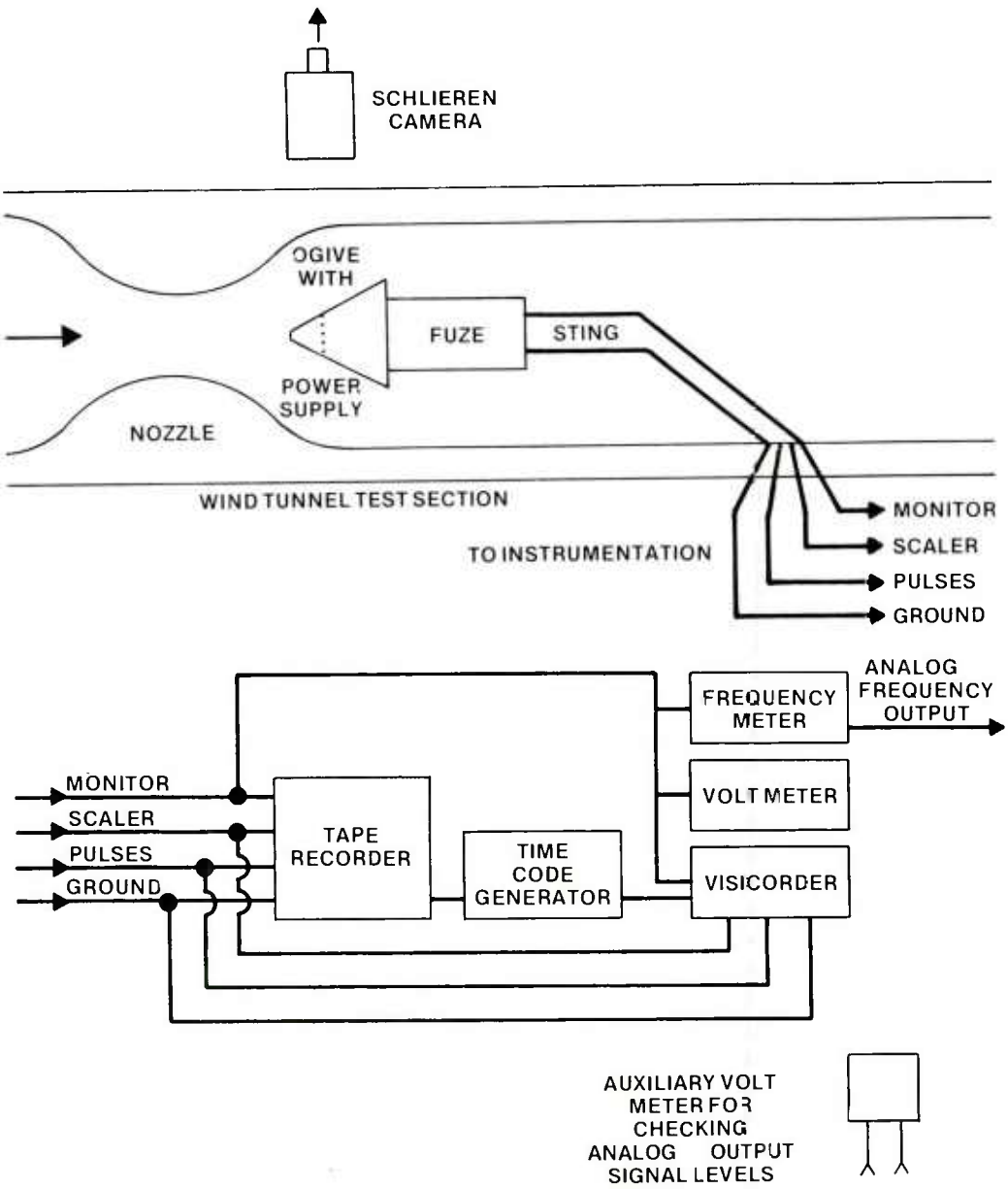

Figure 7. Diagram of apparatus for wind tunnel test.

pressure and temperature. The Mach number was determined by the nozzle block used. The altitude was then computed in terms of the total pressure and the Mach number. The total pressure was increased, and the process was repeated until the range of total pressure values had been covered at that Mach number. A different nozzle block was used for each Mach number.

4. WIND TUNNEL TEST RESULTS

4.1 Fluidic Generator

A portion of the visicorder trace for the run at Mach 1.5 is shown in figure 8. The top trace is the scaler signal, and the trace below is the power supply monitor signal. The total pressure values are indicated. The scaler comes on near 13.7 kPa (2.0 psia). Figure 9(a) plots fuze input voltage, calculated from the measured monitor signal amplitude, versus total pressure at Mach 1.5. This plot shows that the input value of 55 V at which the scaler comes on was achieved at 15.1 kPa (2.2 psia). Similar plots (fig. 9b and 9c) show that the pressure at which the scaler comes on increased to 23.4 kPa (3.4 psia) at Mach 1.76 and 34.4 kPa (5.0 psia) at Mach 2.02.

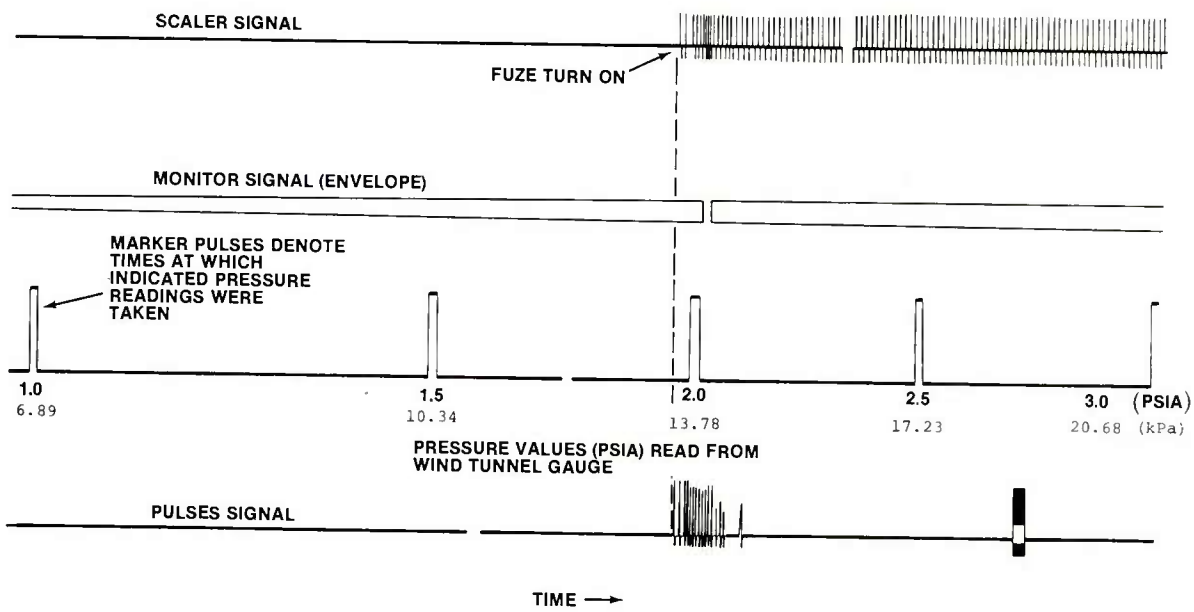

Figure 8. Visicorder record of high frequency fluidic generator during wind tunnel run at Mach 1.5.

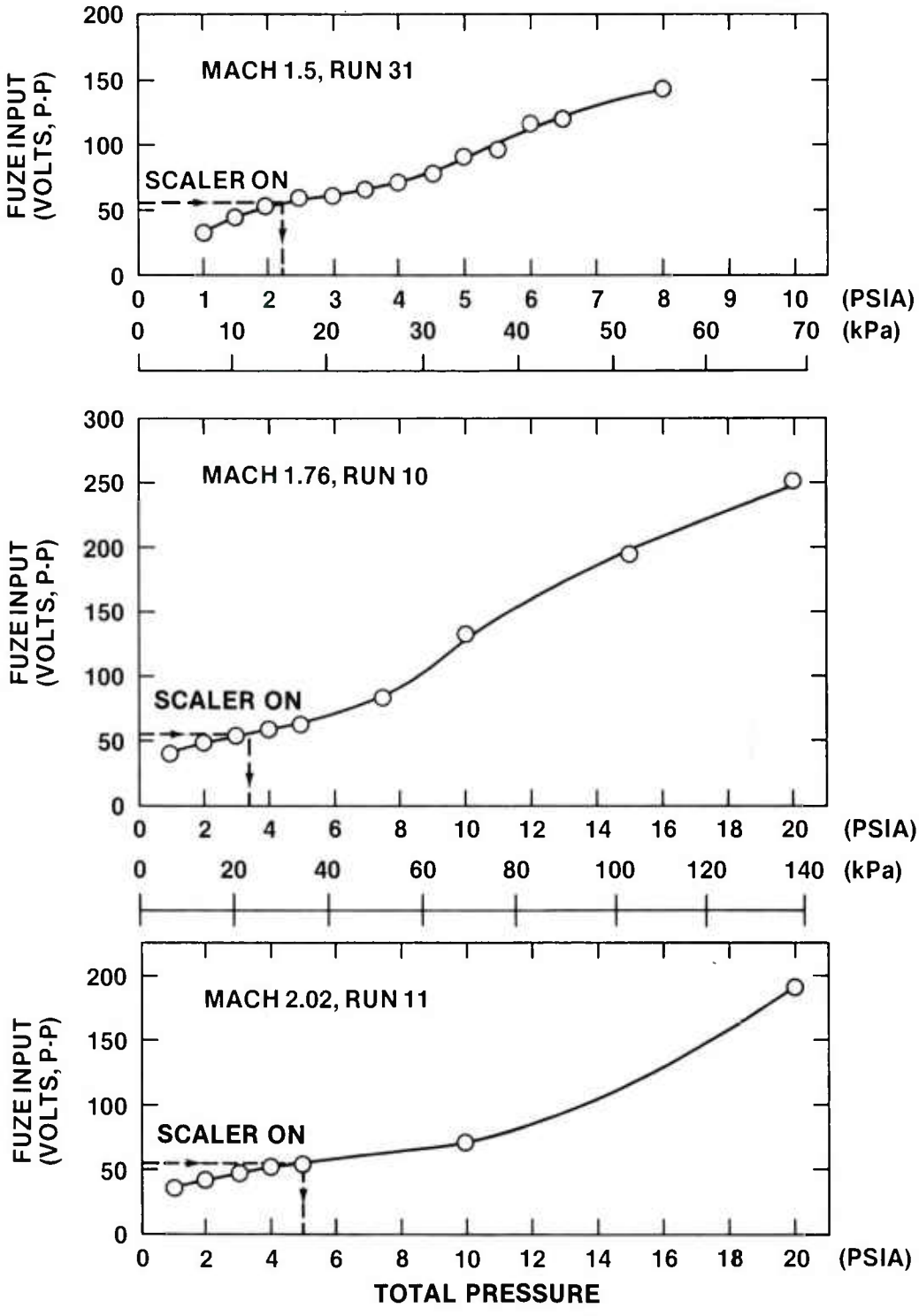

Figure 9. Performance of high frequency fluidic generator in wind tunnel.

The fuze input signal is plotted versus altitude in figure 10. All points fall on the same curve regardless of Mach number. Fuze operation as indicated by the initiation of scaler signal occurs for points above the dashed horizontal line at 55 V.

A comparision of the laboratory data of input voltage versus supply pressure before and after the wind tunnel test (table 1) shows no degradation in the generator output as a result of the wind tunnel testing.

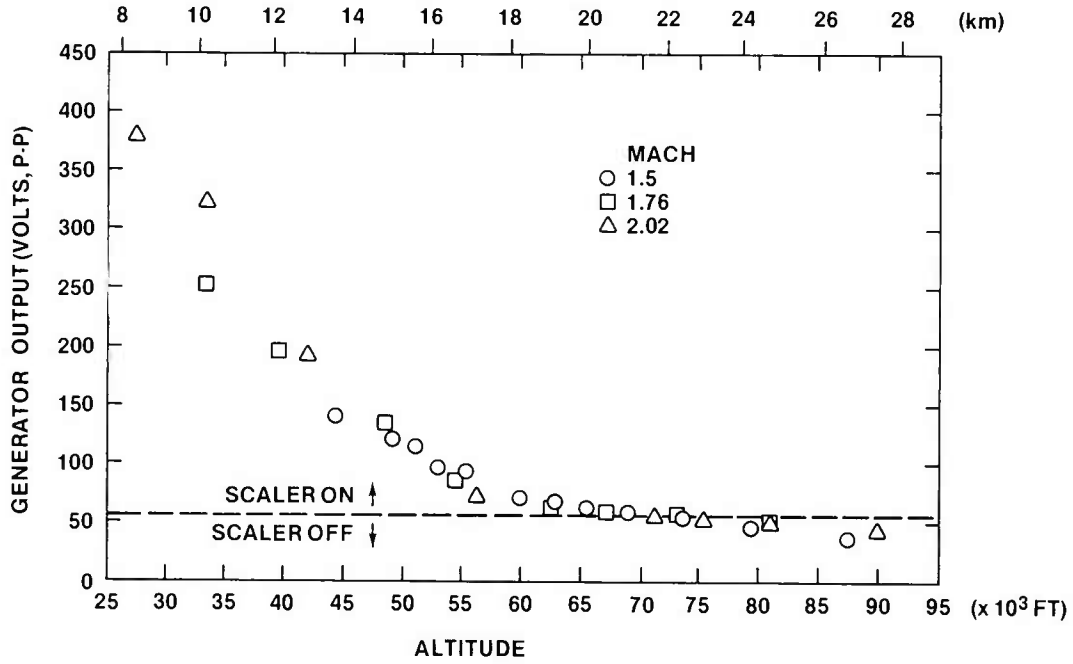

Figure 10. Fuze input voltage versus altitude for high frequency fluidic generator 40.

TABLE 1. COMPARISON OF HIGH FREQUENCY FLUIDIC GENERATOR VOLTAGE OUTPUT BEFORE AND AFTER WIND TUNNEL TEST

Pressure difference from inlet to exhaust ports		Monitor signal (V rms)	
(kPa)	(psig)	Before	After
3.44	0.5	0.080	0.069
6.89	1.0	0.116	0.123
10.3	1.5	0.143	0.170
13.78	2.0	0.170	0.268
20.68	3.0	0.298	0.360

4.2 *Alternator*

A second type of ram air driven power supply was tested in the wind tunnel (fig. 11). The alternator employs an air driven turbine, which spins a permanent magnet that switches the magnetic flux through the stator coil. The alternator was designed for low supply pressure operation, 69 kPa (10 psig) in the laboratory, whereas the equivalent of 724 kPa (105 psig) is encountered at rocket burnout. For the alternator to survive the higher pressure region, a star shaped disk was mounted on the turbine to reduce the flow through the blades and lower the rotational speed at the higher pressures.

To establish the minimum area that would allow the fuze to operate at the high altitudes, two inlet areas were investigated: a venturi having an 8.73×10^{-3} m (0.344 in.)-diameter throat and another having a 6.09×10^{-3} m (0.240 in.)-diameter throat. The smaller diameter inlet limits the flow to the turbine at the velocities at rocket burnout and reduces the stress on the bearings, thus augmenting the effect of the star disk in reducing alternator rotational speed at high projectile velocity.

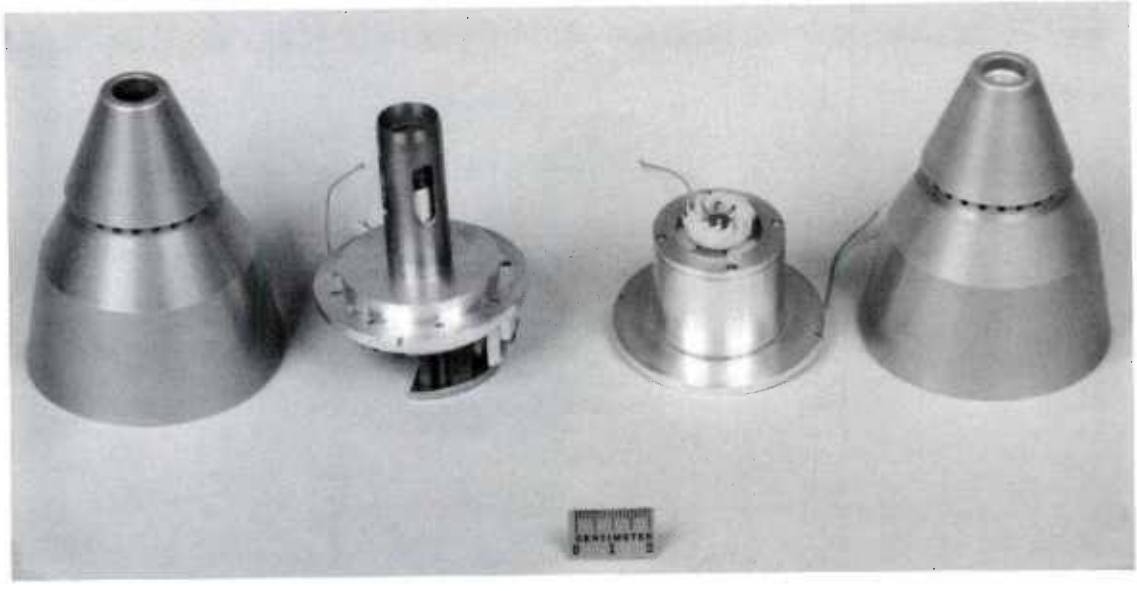

Figure 11. Power supplies used in wind tunnel test.

Figure 12 plots fuze input voltage versus total pressure for three Mach numbers for the larger diameter inlet. For all Mach numbers, the scaler came on below the lowest total pressure data point in the tunnel. The lowest established total pressure at which the fuze operated at Mach 1.5 was 6.89 kPa (1 psia). At Mach 1.76, the lowest pressure was 8.6 kPa (1.25 psia), and at Mach 2.02, the pressure was 10.3 kPa (1.5 psia). The voltage level remained constant at 110 to 120 Vp-p at higher pressures. This limitation in voltage level is imposed by the alternator itself, which is a 2- to 3-W device. Moreover, the electrical load for the MLRS fuze is much higher than that for maximum power transfer.

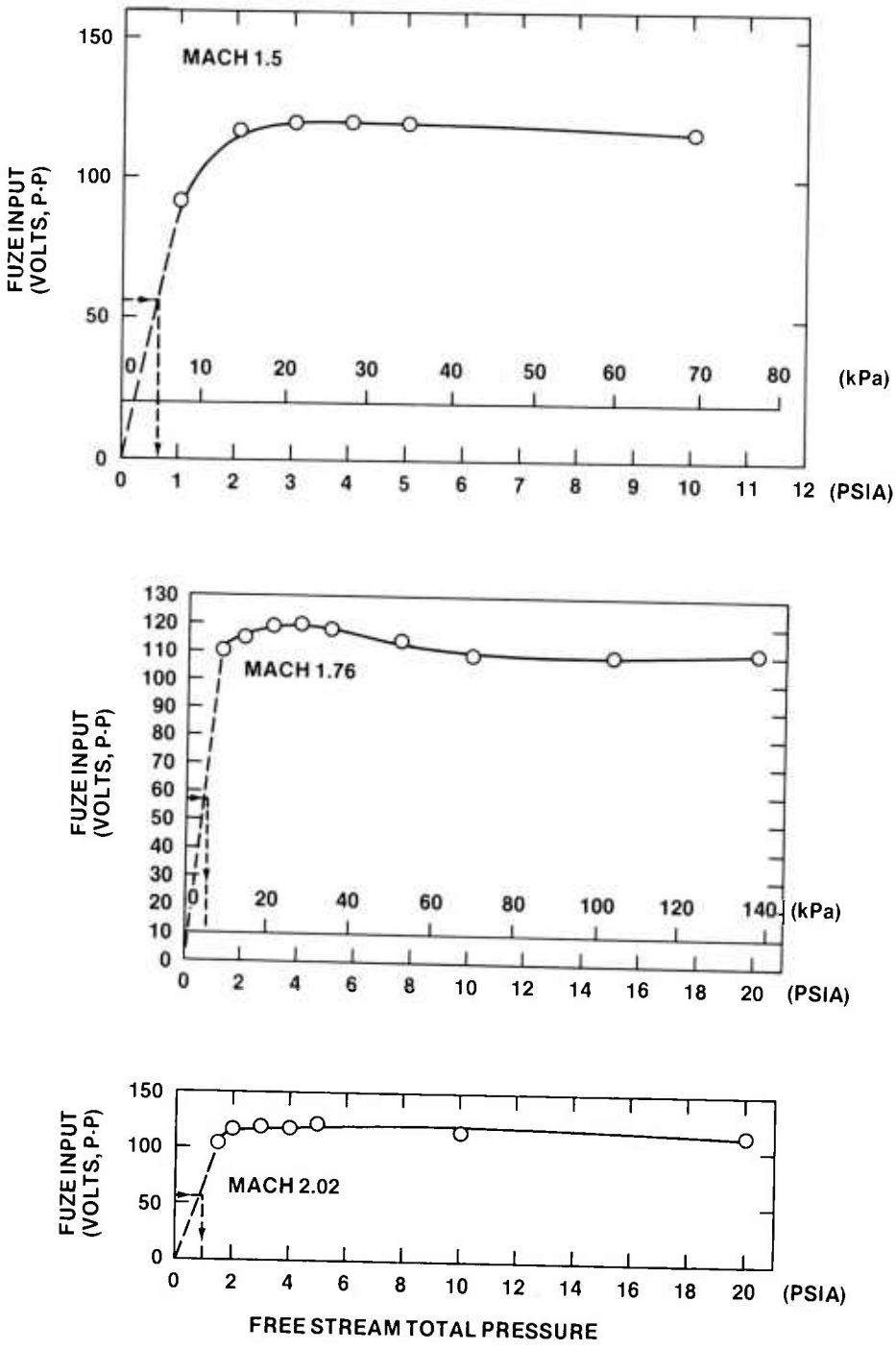

Figure 12. Performance of alternator H-531 in ogive with 8.73 × 10^{-3} m (0.344 in.)-diameter venturi in wind tunnel.

The voltage is plotted versus altitude for the three values of Mach number in figure 13. The 55 V required to operate the fuze is achieved throughout the wind tunnel operation.

A smaller inlet having a 6.09×10^{-3} m (0.240 in.)-diameter venturi section was tested in the wind tunnel with alternator H-536 and ogive with 24 exhaust ports, each 1.93×10^{-3} m (0.076 in.) in diameter. The small inlet is desirable to protect the alternator dur ng the high velocities encountered on the burn phase and earlier portions of the trajectory. The purpose of this test was to determine the effect of the smaller inlet on operation at higher altitudes where pneumatic input is minimal.

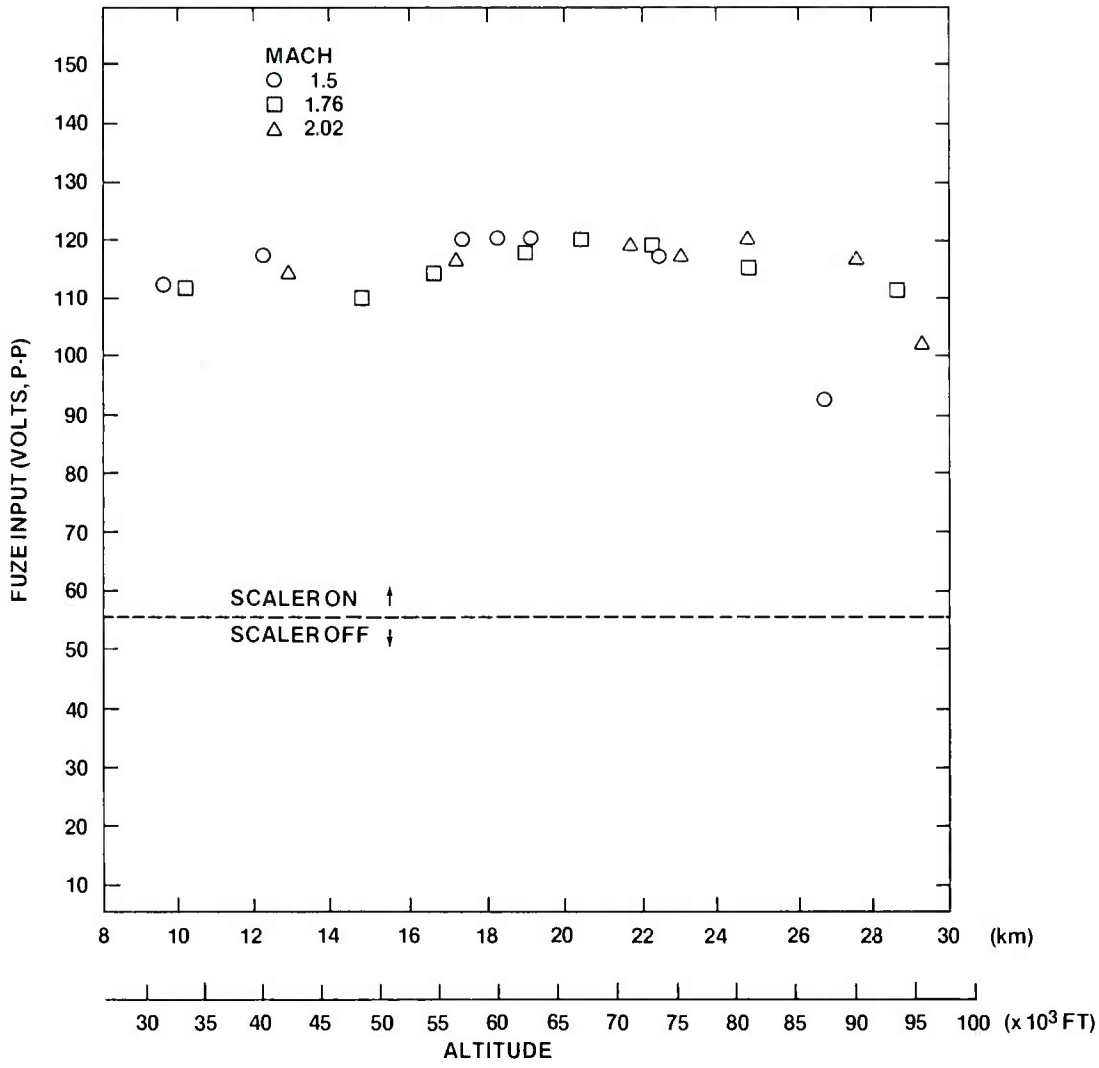

Figure 13. Fuze input voltage versus altitude for alternator H-536 in ogive with 8.73×10^{-3} m (0.344 in.)-diameter venturi.

Figure 14 graphs fuze input voltage versus altitude for the three Mach numbers investigated. The horizontal dashed line denotes the voltage level to operate the fuze. The voltage remains at 110 to 120 V regardless of Mach number up to an altitude of 18.28 km (60,000 ft). Above that altitude, the voltage decreases with altitude. The voltage decreases more with altitude at lower Mach numbers than at higher Mach numbers. Thus, by comparison with figure 13 for the 0.344-in.-diameter inlet, the effect of the smaller inlet is to reduce the operating altitude of the fuze.

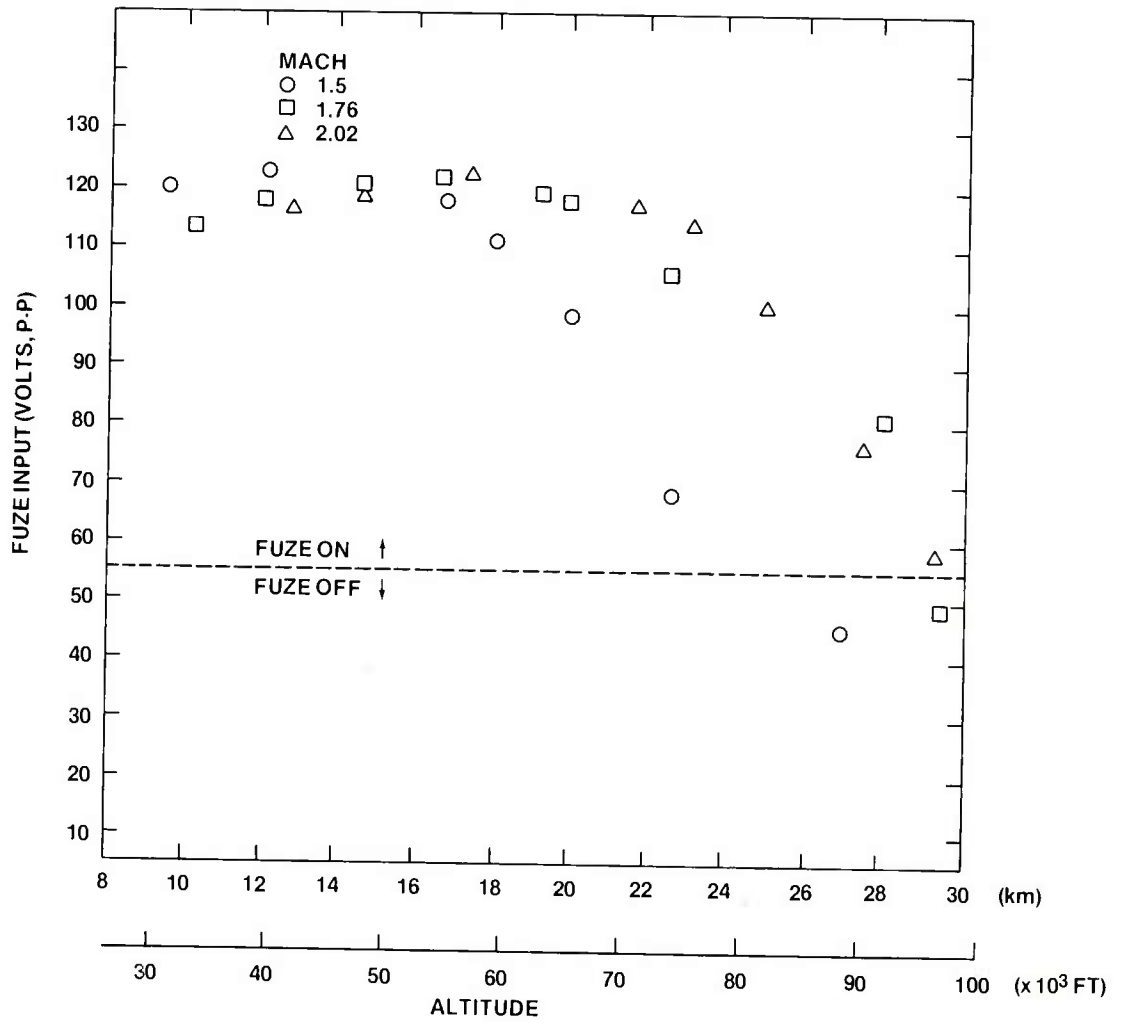

Figure 14. Fuze input voltage versus altitude for alternator H-536 in ogive with 6.10×10^{-3} m (0.240 in.)-diameter venturi.

Table 2 compares the laboratory test of the alternator with the fuze before and after the wind tunnel test. The alternator, even though it was designed for subsonic flow regimes, did not degrade in performance noticeably as a result of the wind tunnel test.

TABLE 2. ALTERNATOR VOLTAGE OUTPUT BEFORE AND AFTER WIND TUNNEL TEST

Pressure difference from inlet to exhaust ports		Monitor signal (V rms)	
(kPa)	(psig)	Before	After
1.37	0.2	0.071	0.064
3.44	0.5	0.142	0.130
4.82	0.7	0.178	0.157
6.89	1.0	0.215	0.197

4.3 Summary of Wind Tunnel Results

The fluidic generator output was higher at lower altitudes for the Mach number conditions tested. As altitude increased, the generator output dropped, but produced sufficient voltage to operate the fuze up to 18.28 km. From 18.28 km to 21.33 km (70,000 ft), the output was marginal. Above 21.33 km, the generated voltage fell below the 55 V required to operate the fuze. Although the alternator did not reach values of 250 to 350 V at altitudes below 10 km (35,000 ft), it did produce more than 90 V, which is sufficient voltage to operate the fuze over the altitude range of the wind tunnel test from 8.22 km (27,000 ft) to 27.4 km (90,000 ft).

5. EVALUATION OF FLUIDIC GENERATOR OUTPUT NEAR APEX OF HIGH ALTITUDE TRAJECTORY

Not all conditions of Mach number and altitude obtained in the wind tunnel correspond to conditions achieved in actual flight. The purpose of this section is to use the data from the wind tunnel test to infer the operation of the fluidic generator along the high altitude portion of the trajectory having the least pneumatic input power to the fluidic generator.

5.1 Relationship of Trajectory to Wind Tunnel Profile

The rocket high altitude trajectory (to be partially simulated in the wind tunnel) is shown in figure 15, in which altitude is plotted versus horizontal range. The flight Mach number and the total pressure are indicated at various points. Near the apex, the rocket achieves a maximum altitude of 19 km (62,500 ft) and minimum Mach number = 1.39. The trajectory is plotted in terms of the wind tunnel parameters of Mach number versus altitude in figure 16. The Mach number range of the trajectory is from 1.39 to 2.72, and the altitude varies from 3.048 km (10,000 ft) at firing to 19 km at the apex.

In figure 17, the conditions attainable in the wind tunnel are shown on a plot of Mach number versus altitude. The conditions fall along lines of constant Mach number that correspond to the nozzle blocks available for use in the tunnel.

When the curves in figures 16 and 17 are plotted on the same graph, the points of intersection (indicated by "o") are the tunnel conditions that correspond to the indicated points along the MLRS flight trajectory (fig. 18).

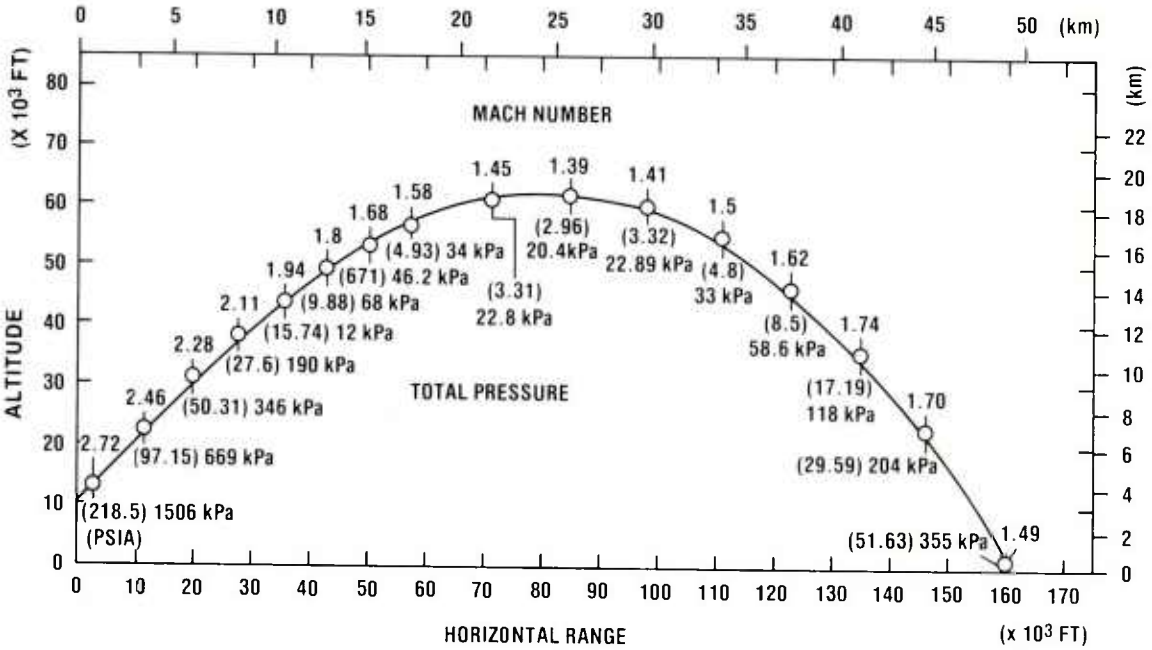

Figure 15. High altitude trajectory with quadrant elevation = 50 deg.

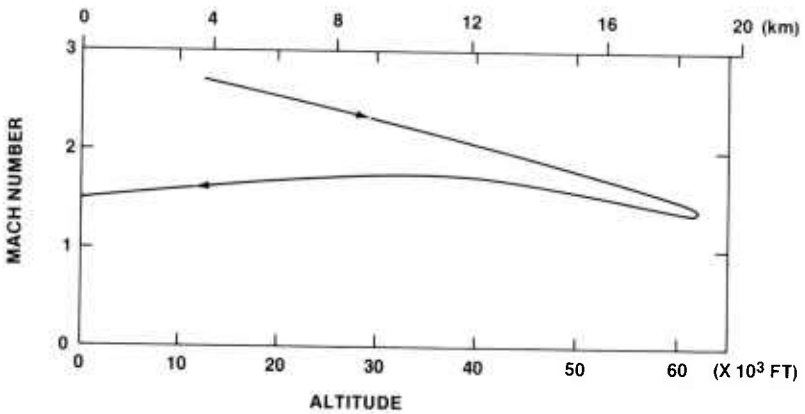

Figure 16. Variation of Mach number with altitude on trajectory with quadrant elevation = 50 deg and initial altitude = 3.048 km (10,000 ft).

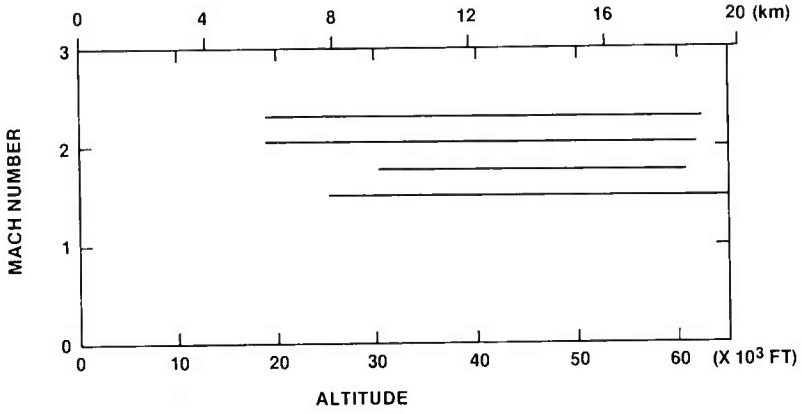

Figure 17. Conditions of Mach number and altitude obtainable in wind tunnel.

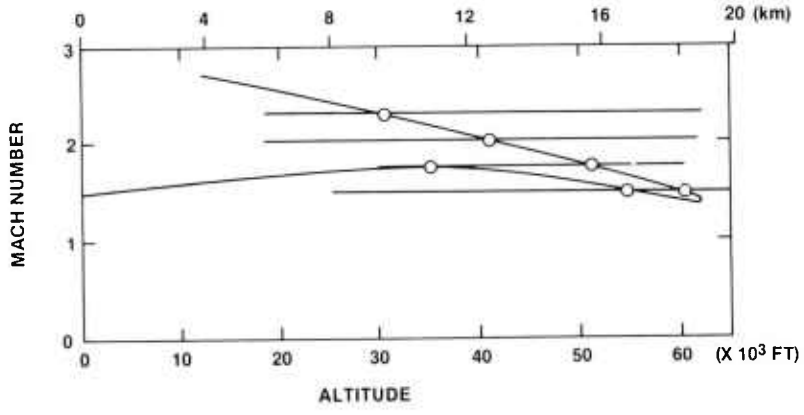

Figure 18. Trajectory conditions obtainable in wind tunnel.

5.2 Test Procedure

During the wind tunnel test, total pressure, total temperature, and fuze monitor signal were observed. The Mach number was established by the nozzle block used. The altitude was then computed in terms of total pressure, temperature, and Mach number.

5.3 Test Results

The voltage generated at each of the trajectory conditions by the fluidic generator is shown in table 3. These points are plotted also on the high altitude trajectory in figure 19.

It is apparent from figure 18 that the conditions of altitude and Mach number at the apex cannot be fully simulated with the Mach 1.5 nozzle. The total pressure at the apex is 20.6 kPa (3 psia) at Mach 1.39 (fig. 15). The total pressure of 20.6 kPa at the apex can be obtained by operating the tunnel at an altitude of 19.8 km (65,000 ft), even though the Mach 1.5 nozzle is used. The voltage value obtained at 20.6 kPa, Mach 1.5, and 19.8 km is 60 Vp-p.

TABLE 3. FUZE INPUT VOLTAGE FROM HIGH FREQUENCY FLUIDIC GENERATOR AT POINTS ON HIGH ALTITUDE TRAJECTORY

Mach No.	Altitude		Fuze input voltage (Vp-p)
	(km)	(ft)	
2.02	12.5	41,000	200
1.76	15.6	51,300	105
1.50	18.4	60,500	70
1.50	16.67	54,700	91
1.76	10.66	35,000	238

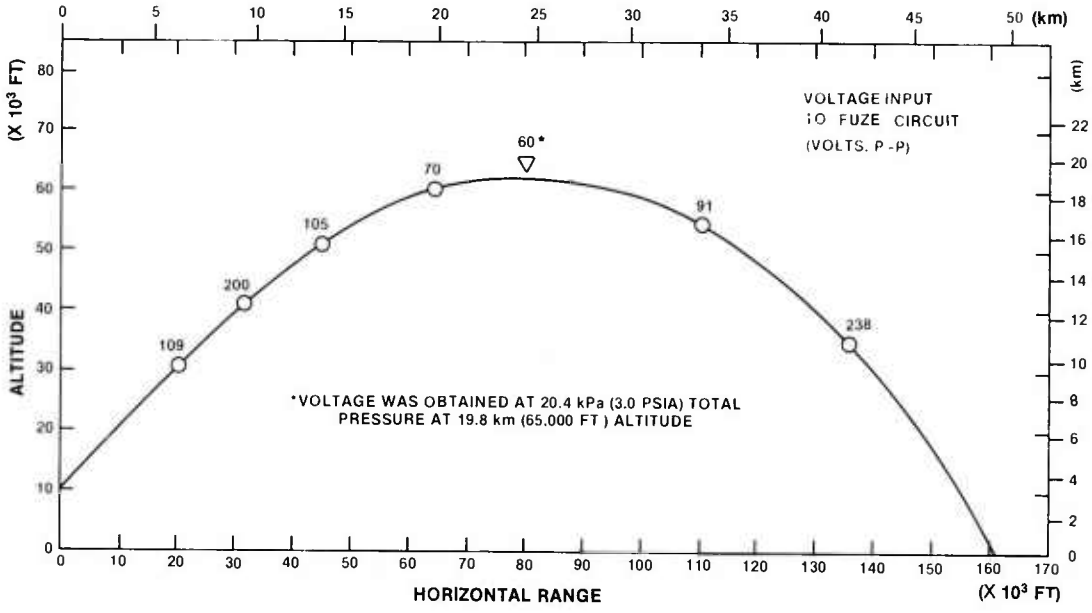

Figure 19. Fuze input voltage measured in wind tunnel at points of high altitude trajectory by using high frequency fluidic generator.

The conditions of Mach number and altitude for the apex of several other trajectories planned for the MLRS rocket are shown in table 4. The total pressure calculated for these points also is shown. These Mach numbers could not be achieved in the wind tunnel, but the range of total pressure was obtained during the run at Mach 1.5. The expected voltages are obtained from figure 9, in which voltage is a function of total pressure at Mach 1.5 for high frequency fluidic generator 40. The expected voltage values at these trajectory points are included in table 4.

TABLE 4. EXPECTED FUZE INPUT VOLTAGE FROM HIGH FREQUENCY FLUIDIC GENERATOR AT TRAJECTORY POINTS PLANNED FOR MLRS ROCKET

Mach No.	Altitude		Free stream total pressure		Expected fuze input voltage* (Vp-p)
	(km)	(ft)	(kPa)	(psia)	
1.15	13.1	43,000	36.8	5.35	97
1.24	14.9	49,000	31.0	4.50	78
1.37	18.8	62,000	20.3	2.95	60
1.12	15.8	52,000	23.4	3.40	64
1.24	18.8	62,000	17.0	2.47	58

**Expected voltage obtained from high frequency fluidic generator wind tunnel data voltage versus total pressure at Mach 1.5.*

6. SELECTING WIND TUNNEL PARAMETER TO ASSESS POWER SUPPLY PERFORMANCE

The aim of this section is to select a useful flow parameter that is obtainable from wind tunnel, flight, and laboratory data to describe power supply performance. The method is to examine the measured wind tunnel fuze input voltage values as a function of various flow parameters that can be measured directly in the wind tunnel or that can be calculated from measured quantities. The parameter that most completely describes the voltage data is sought.

In figure 9, fuze input voltage for the high frequency fluidic generator is plotted versus total pressure measured in the wind tunnel. The relationship depends on Mach number.

In figure 10, voltage is plotted versus altitude, and the relationship is less dependent on Mach number, especially at the higher altitudes. The altitude is obtained from standard atmospheric tables of static pressure versus altitude, where the static pressure had been calculated from measured values of total pressure and Mach number.

In figure 20, voltages are plotted versus free stream dynamic pressure, q_1, for the several Mach numbers. Voltage is clearly a function of Mach number. The free stream dynamic pressure is readily calculated in terms of Mach number and total pressure.

These free stream flow parameters of Mach number, total pressure, altitude, and free stream dynamic pressure can all be obtained from radar and atmospheric data on trajectories of rocket projectiles. The radar measures velocity and position including range, lateral displacement, and altitude of the projectile, which appears as a point on the radar screen. Static pressure and temperature at the various altitudes are obtained from standard atmospheric tables. From this information, the free stream flow parameters can be calculated as in the wind tunnel. Because the spatial resolution of the radar is inadequate to determine the shape of the projectile, the flow pattern past the projectile cannot be obtained. The flow pattern, which is a primary factor in assess-

ing the pneumatic energy available to fuzes powered with ram air energy, is readily studied from shadowgraph and Schlieren photographs taken in the wind tunnel (fig. 21).

These figures show a bow shock in front of the projectile. This flow pattern is discussed in a recent wind tunnel report.[1] The dynamic pressure at the ogive inlet, q_2, is different from the free stream dynamic pressure, q_1, ahead of the bow shock and can be calculated in terms of the Mach number and total pressure.

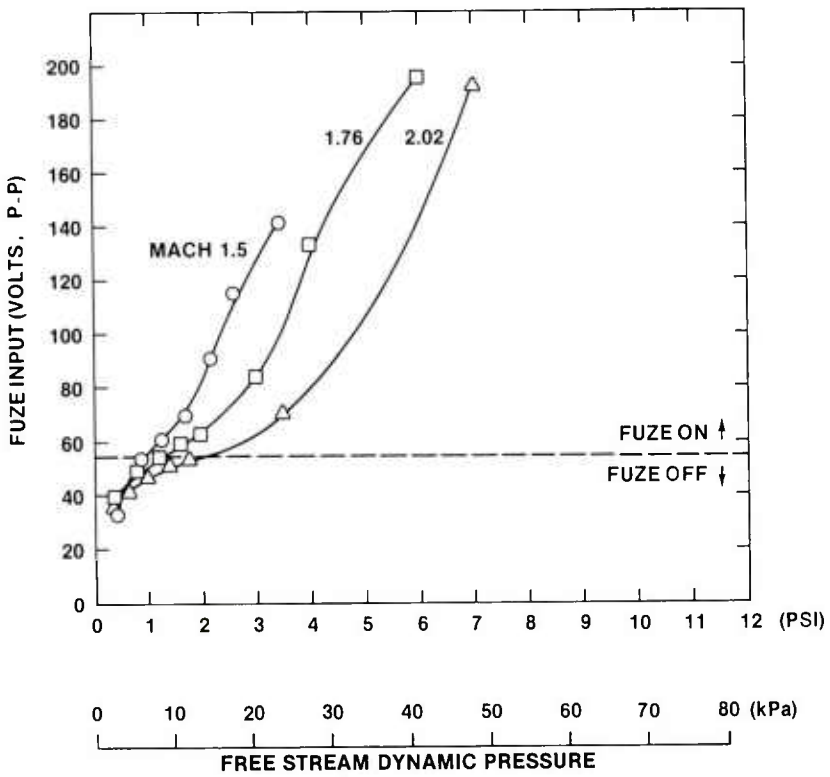

Figure 20. Fuze input voltage in wind tunnel versus free stream dynamic pressure for high frequency fluidic generator 40.

The following formulae, which are obtained from the literature,[2] are used to calculate q_1 and q_2:

$$q_1 \equiv (1/2)\rho_1 v_1^2 = (\gamma/2)\,(p_1/p_{t1})p_{t1}M_1^2 \quad , \qquad (1)$$

[1] *Jonathan E. Fine, Analysis of Wind Tunnel Test Results of Fluidic Generator for High-Altitude Rocket, Harry Diamond Laboratories HDL-TR-1877 (March 1979).*

[2] *Ames Research Staff, Equations, Tables, and Charts for Compressible Flow, National Advisory Committee for Aeronautics Report 1135, U.S. Government Printing Office, Washington, DC (1953).*

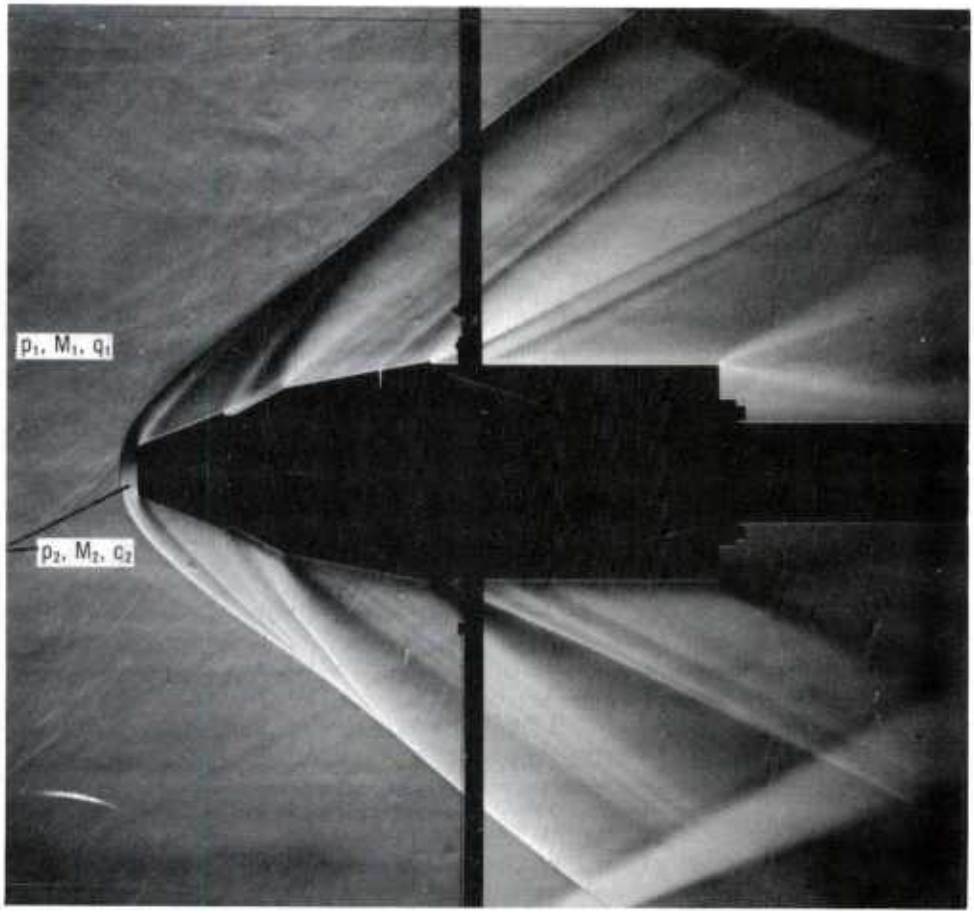

Figure 21. Schlieren photograph of ogive at Mach 2.02

where ρ_1 is the static density of the atmosphere v_1 is the projectile velocity, γ is the ratio of specific heats (1.4 for air), p_1 is the free stream static pressure, p_{t1} is the free stream total pressure, and M_1 is the free stream (or flight) Mach number.

$$q_2 \equiv (1/2)\rho_2 v_2^2 = (\gamma/2)(p_2/p_1)\left(p_1/p_{t1}\right)p_{t1}M_2^2 \quad , \tag{2}$$

where ρ_2 and v_2 are, respectively, the static density and the velocity behind the bow shock, p_2 is the static pressure, and M_2 is the Mach number behind the shock.

The ratios (p_1/p_{t1}) and (p_2/p_1) and M_2 are functions only of Mach number M_1 and can be obtained from compressible flow tables.[2]

Both q_1 and q_2 are plotted in figure 22 as a function of the free stream total pressure for the three values of Mach number studied in the wind tunnel. At a given total pressure, the variation in q_2 with Mach number is greater than the corresponding variation of q_1.

[2]*Ames Research Staff, Equations, Tables, and Charts for Compressible Flow, National Advisory Committee for Aeronautics Report 1135, U.S. Government Printing Office, Washington, DC (1953).*

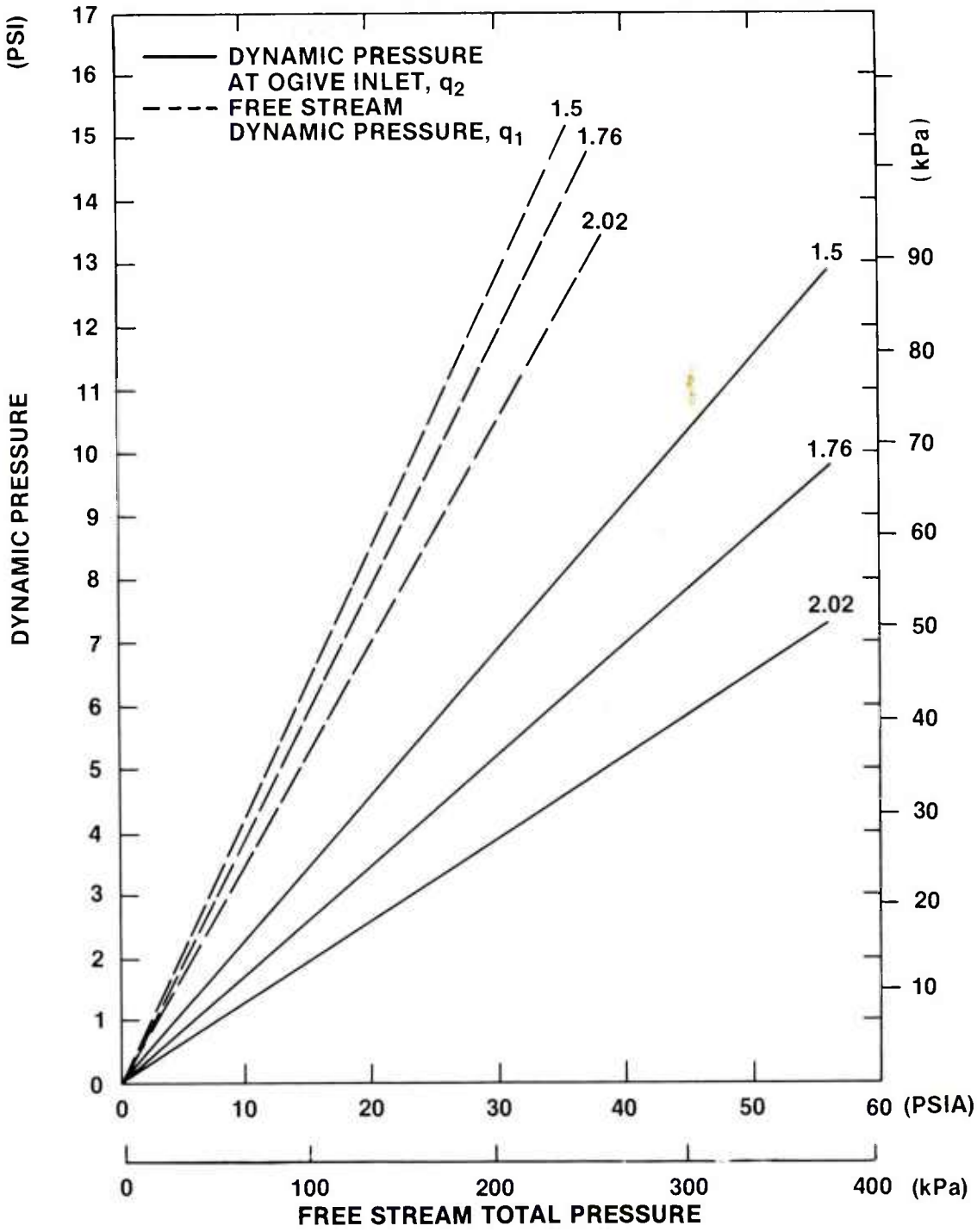

Figure 22. Free stream dynamic pressure as function of total pressure in wind tunnel at Mach numbers tested.

The fuze input voltage from the high frequency fluidic generator is plotted in figure 23 versus the dynamic pressure at the ogive inlet for the wind tunnel Mach numbers. The voltage is independent of Mach number over the range of the wind tunnel test. Thus, q_2 is a useful independent variable for describing the variation of fuze input voltage in the wind tunnel.

In figure 24, the fuze input voltage is plotted versus q_2 for the alternator having the 8.73×10^{-3} m (0.344 in.)-diameter venturi. The voltage is independent of Mach number, as with the fluidic generator, even though the shape of the voltage versus q_2 curve is different for each of the two kinds of power supply.

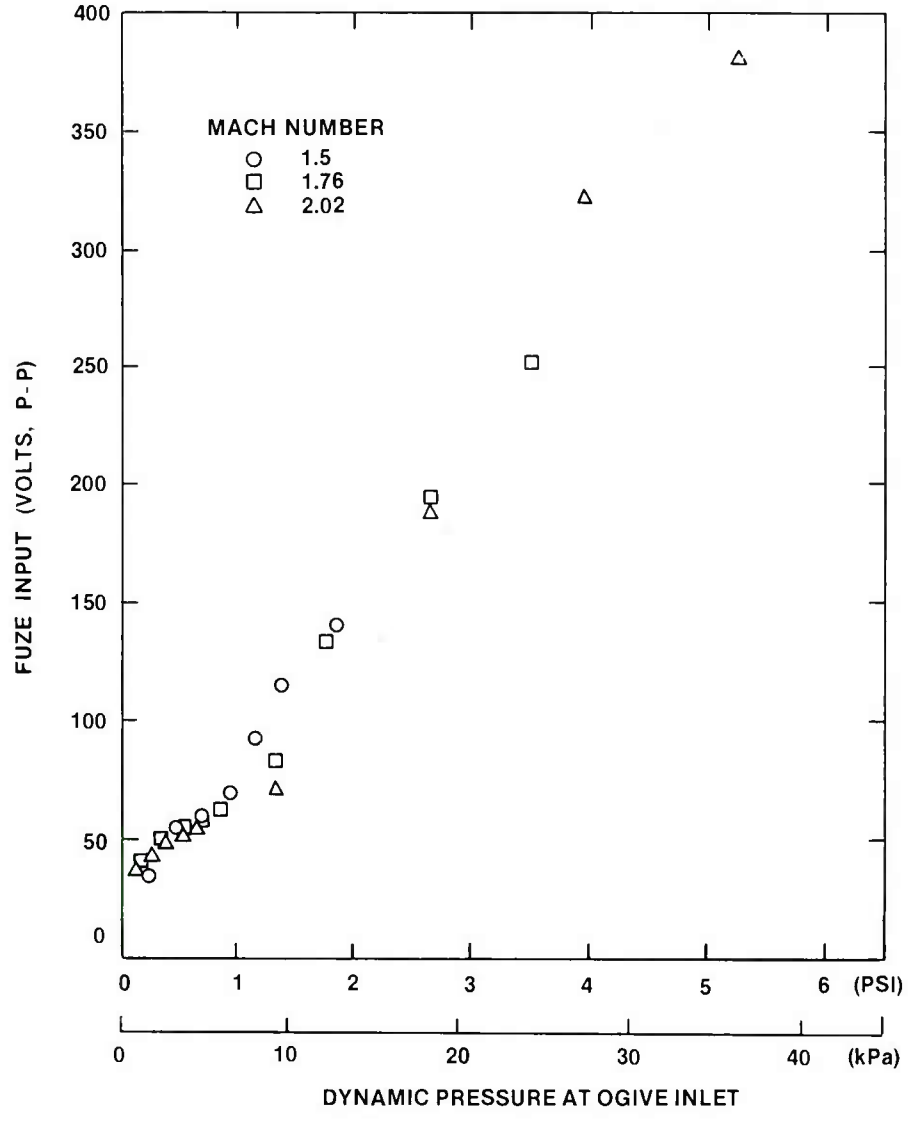

Figure 23. Fuze input voltage provided by high frequency fluidic generator 40 versus dynamic pressure at ogive inlet.

From figures 23 and 24, it appears that in the wind tunnel the dynamic pressure at the ogive inlet is a useful independent variable for describing the output of both the fluidic generator and the alternator power supplies. Its importance can be seen in figure 25, in which q_2 is plotted versus Mach number for various altitudes. This curve applies to both wind tunnel and flight conditions since the static pressures at a given altitude are the same in the wind tunnel or in flight. Note that q_2 itself depends on both Mach number and altitude. However, if a line is drawn as shown at constant value of q_2, the power supply voltage will be the same, even though both Mach number and altitude vary along the line over a wide range.

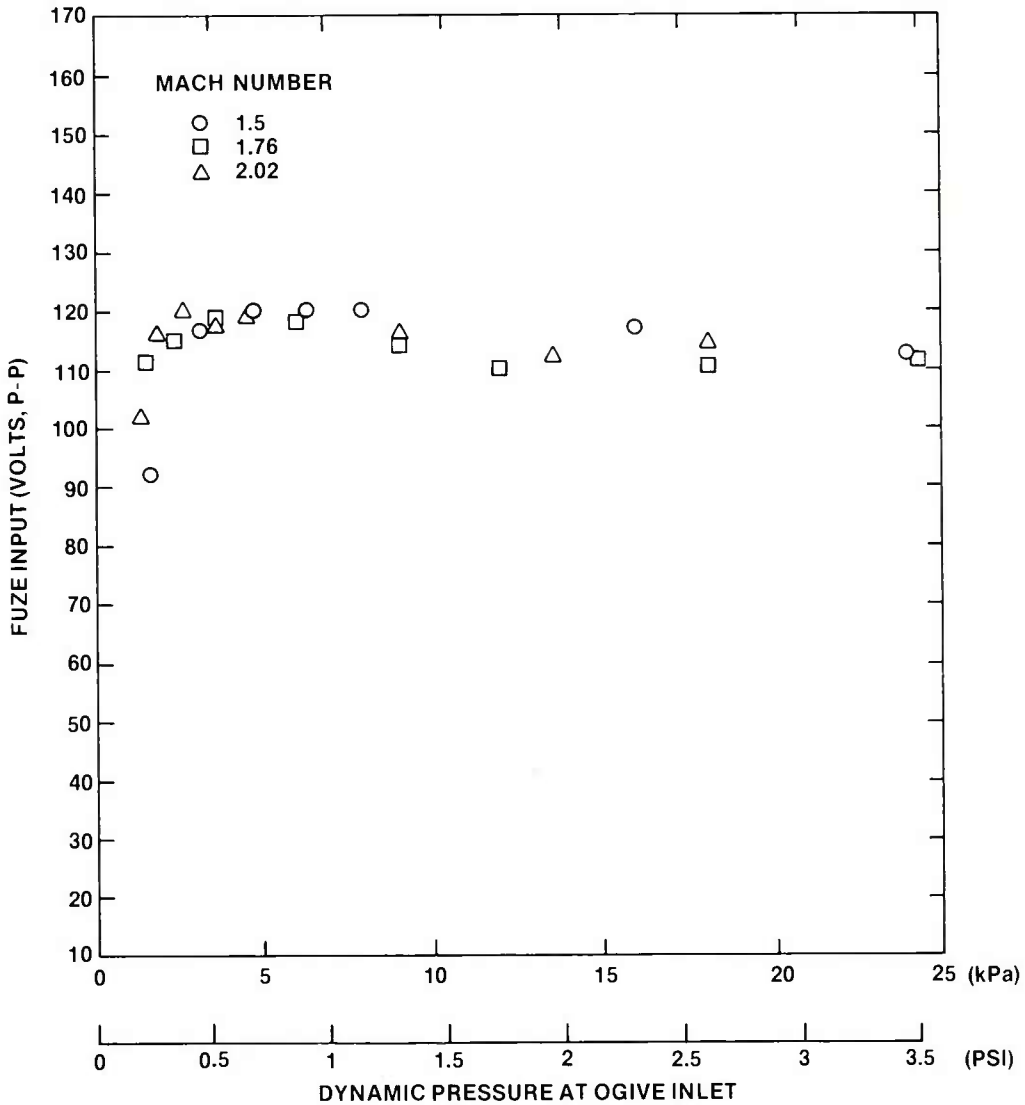

Figure 24. Fuze input voltage provided by alternator H-536 versus dynamic pressure at ogive inlet.

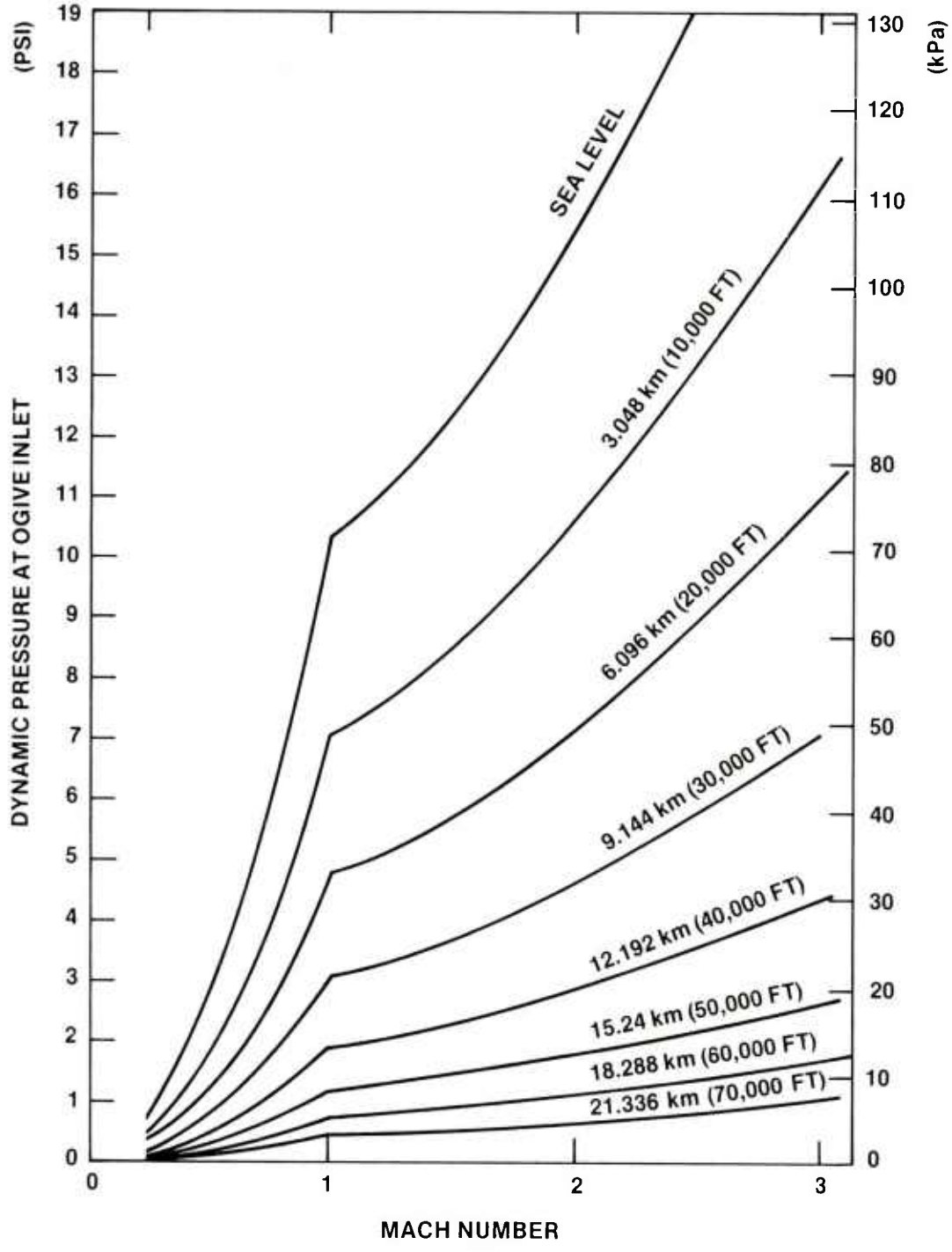

Figure 25. Dynamic pressure at ogive inlet as function of free stream Mach number and altitude.

It is necessary to show how q_2 can be determined for laboratory conditions and used to estimate voltage values in the wind tunnel and in flight.

7. RELATING LABORATORY VOLTAGE DATA TO WIND TUNNEL CONDITIONS

7.1 Wind Tunnel Conditions

The following method is used to relate laboratory conditions to wind tunnel and flight conditions.

Consider first the laboratory test apparatus shown in figure 5. The ogive inlet is connected to a settling chamber, which may be pressurized to any desired value of the supply pressure, p_{sup}. The pressure at the exhaust ports is p_∞, or atmospheric static pressure. The pressure difference from the inlet to the exhaust ports is $(p_{sup} - p_\infty)$.This pressure difference drives the air through the power supply in the laboratory and is assumed to be the same pressure difference that drives air through the power supply in flight or in the wind tunnel.

The pressure difference is a parameter of the air flow external to the ogive and the power supply. Consequently, its use requires no flow fields to be calculated inside the ogive.

From the previous discussion, a bow shock replaces the settling chamber for wind tunnel or flight. The atmospheric pressure, p_∞, in the laboratory therefore is assumed to correspond to the static pressure, p_2, behind the bow shock. The laboratory pressure, p_{sup}, is assumed to correspond to p_{t2}, the total pressure behind the bow shock. Laboratory pressures for which $p_\infty/p_{sup} > 0.52828$ correspond to subsonic flow behind the bow shock. The Mach number, M_2, behind the bow shock therefore may be obtained from the subsonic flow tables and the given pressure ratio. The equivalent flight Mach number, M_1 , is obtained from the supersonic flow tables by looking up the value of M_1 that corresponds to that value of M_2. The corresponding dynamic pressure at the ogive inlet is then q_2, which is obtained by

$$q_2 = (\gamma/2)p_\infty M_2^2 \quad . \tag{3}$$

For subsonic projectile flight, the bow shock is absent, and the pressures and the Mach number become analogous to the free stream values so that

$$M_2 = M_1$$

and

$$q_2 = q_1$$

Hence, the corresponding dynamic pressure at the ogive inlet is given by

$$q_2 = q_1 = (\gamma/2)p_\infty M_1^2 \quad . \tag{4}$$

Two limitations to this method should be kept in mind. First, for laboratory pressures for which $p_\infty/p_{sup} \leqslant 0.52828$, the flow within the generator may be supersonic so that the analogy between laboratory and flight flow patterns is ambiguous. A second limitation is that the exhaust port pressure in flight or in the wind tunnel may be lower than the static pressure because of the external flow past the ogive. This would result in measured voltage values higher than estimated.

In figure 26, dynamic pressure at the ogive inlet has been plotted versus pressure difference for the laboratory arrangement of figure 5. Thus, it is necessary only to refer to figure 26 to obtain the value of q_2 corresponding to a measured pressure value.

A laboratory calibration curve of fuze input voltage for the specified fluidic generator versus q_2 has been obtained as described above and is included in figure 27. This curve applies to the particular fuze and fluidic generator used in the wind tunnel test. A similar curve must be obtained experimentally as indicated for each fluidic generator-fuze system for which expected wind tunnel or flight voltages are required.

The values of q_2 were calculated for the wind tunnel test as a function of total pressure for each Mach number. The expected voltage values were read from the curve of figure 27 and were plotted versus total pressure in figure 28. The measured voltages show good agreement with the expected values, but are higher than predicted, possibly as a result of lower static pressures at the exhaust ports.

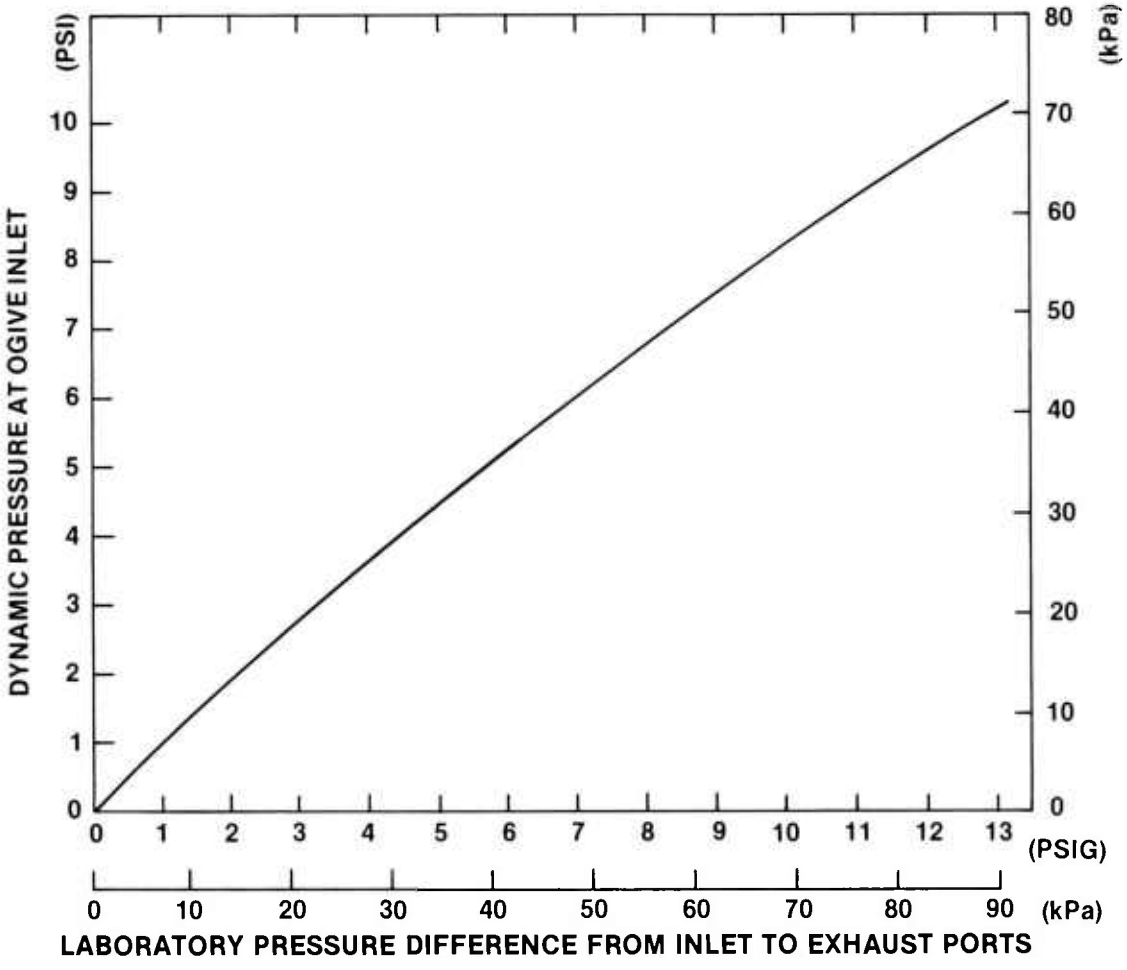

Figure 26. Dynamic pressure at ogive inlet at sea level versus supply pressure in laboratory (atmospheric pressure at exhaust ports is 14.7 psia—101.35 kPa).

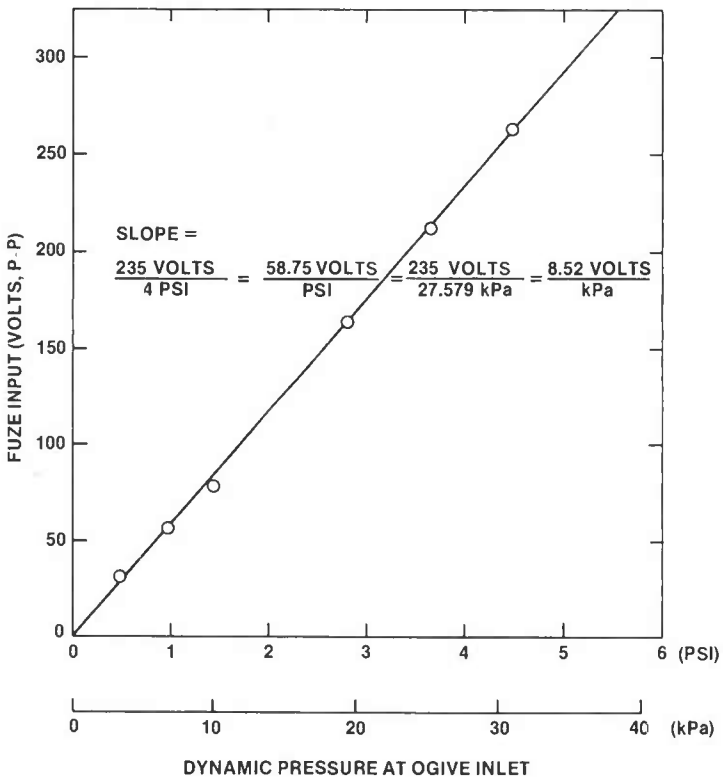

Figure 27. Laboratory calibration curve for high frequency fluidic generator 40.

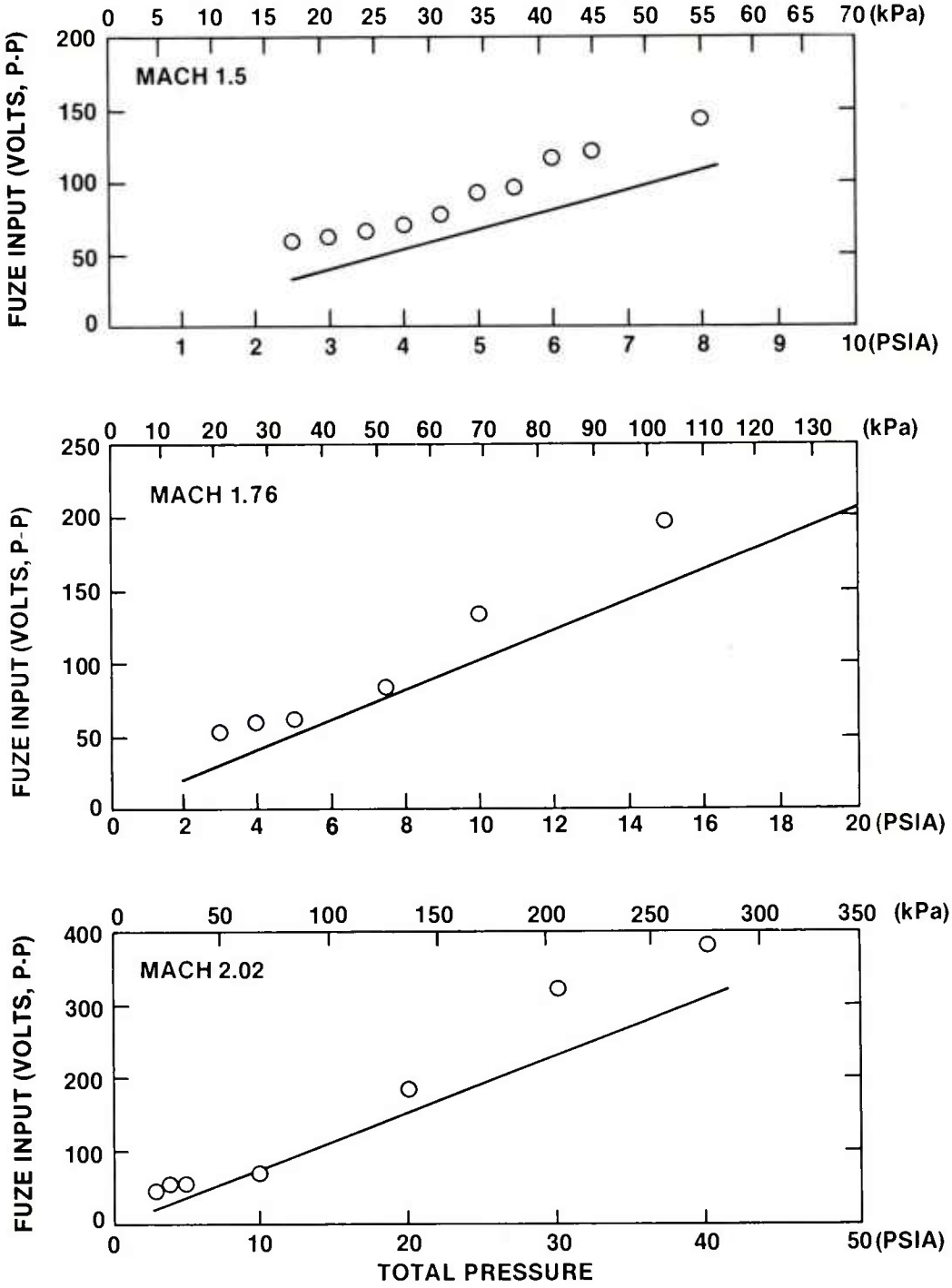

Figure 28. Expected (—) and measured (o) voltage provided by high frequency fluidic generator versus dynamic pressure at ogive inlet.

7.2 Flight Conditions

The method was used to estimate the fuze input voltage along the trajectory of a ZAP round from a recent field test by Richard Goodyear of the Harry Diamond Laboratories. The trajectory obtained from radar data is shown in figure 29. The solid line is a plot of projectile velocity (read along the left vertical axis) versus time from first motion. The dashed line represents altitude (referred to the right hand vertical scale) versus time of flight. The rocket reached a maximum velocity at burnout of the rocket motor of 945 m/s (3100 ft/s) at 1.3 s. The velocity decreased to a minimum at apogee of 122 m/s (400 ft/s) and increased to a value of 381 m/s (1250 ft/s) before impact at 111 s. The rocket was fired from sea level and at apogee reached an altitude of 14.3 km (47,000 ft).

The variation of q_2 versus time along this trajectory is shown in figure 30. It is clear that q_2 closely follows the rocket velocity throughout the flight.

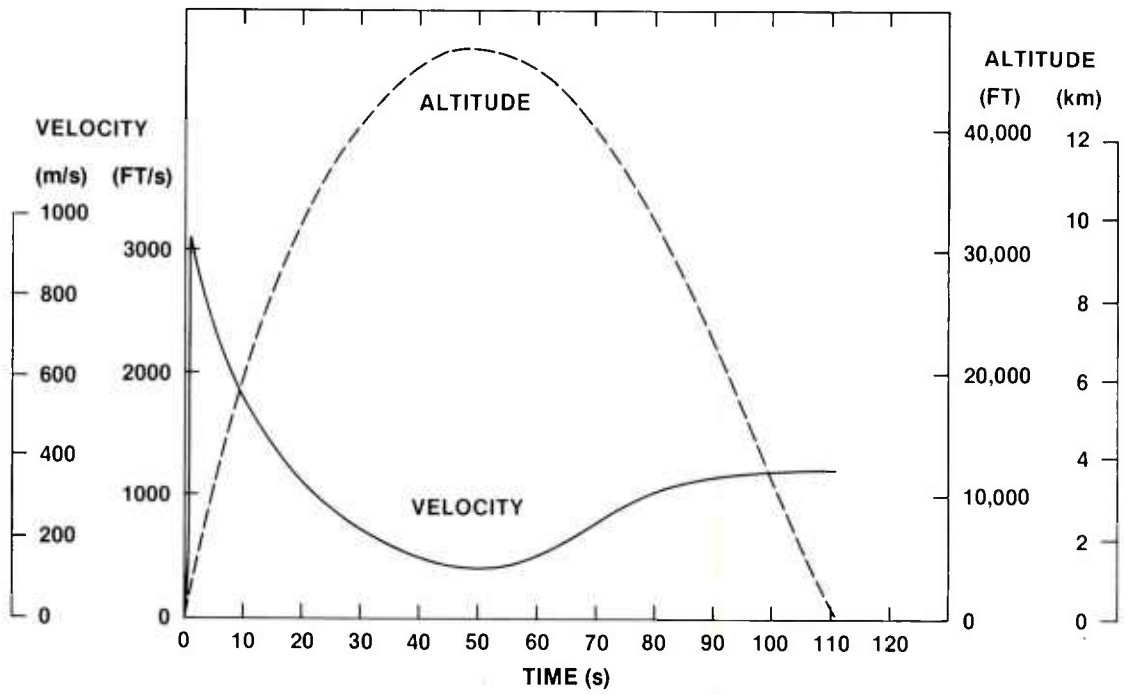

Figure 29. ZAP rocket trajectory, round 9, fuze 79, quadrant elevation = 75 deg, at Wallops Island, VA, field test.

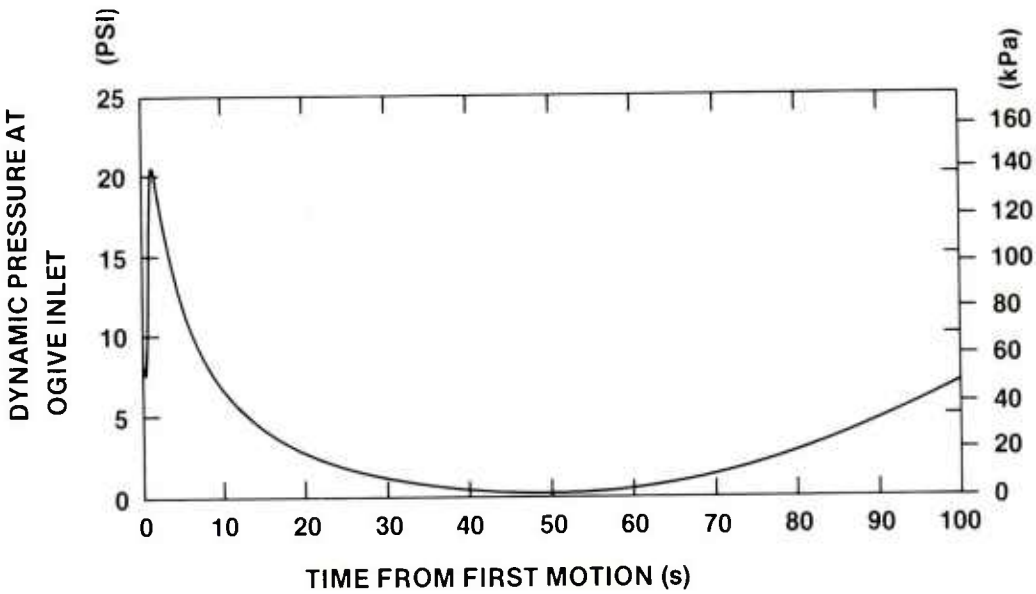

Figure 30. Variation of dynamic pressure at ogive inlet during flight of ZAP rocket, round 9, fuze 79, at Wallops Island, VA, field test.

In the latter portion of the flight, q_2 increases as a result of the increasing air density on the downward leg of the trajectory even though the velocity remains constant.

The laboratory calibration curve of fuze input voltage versus q_2 is included in figure 31 for the fluidic generator-fuze-telemetry system used in the field test. This figure is used to obtain expected voltages in flight just as figure 27 is used to obtain expected voltages in the wind tunnel.

The expected voltage values obtained from figure 31 for the values of q_2 from figure 30 are plotted versus time of flight along the solid curve of figure 32. The dashed portion represents the low pressure region for which laboratory data were not obtained. The flight voltage data follow the predicted curve, but are higher than expected over most of the trajectory. As with the wind tunnel data, the discrepancy may arise from not considering the enhancing effect of flow over the ogive in flight. However, the large values over the first several seconds of flight are believed to result from stagnation temperatures in flight that reach nearly 555 K (1000 R) at burnout, as compared with 288 K (519 R) in the laboratory or 311 K (560 R) in the wind tunnel. The effects of these departures from laboratory temperature conditions are discussed in the GSRS-6 Field Test Report. The method presented does serve as a low estimate of voltage obtained in the field test.

The ZAP trajectory when plotted with available wind tunnel conditions on a chart of Mach number versus altitude (fig. 33) shows that three points on the trajectory corresponded to conditions obtainable in the wind tunnel. These points occurred at 7, 10, and 14 s into the flight. From figure 32, the agreement between the expected and measured values is good at these three points.

In the same field test, a fluidic generator powered fuze was flown on a Zuni rocket, which followed the trajectory of figure 34. The maximum velocity occurred at 1.3 s, and the maximum altitude was 4.08 km (13,400 ft), much lower than for the ZAP. The dynamic pressure at the ogive inlet (fig. 35) follows the velocity, as for the ZAP. The same laboratory data used for the ZAP calibration curve (fig. 35) furnished the expected voltage values that are plotted versus time in figure 36. The measured values also are shown. The measured voltage follows the expected curve as for the ZAP. The measured voltages in the first few seconcs of flight are still much higher than expected; however, the values through the rest of the flight are in gcod agreement with the prediction. The method furnishes better agreement over the lower altituce trajectory.

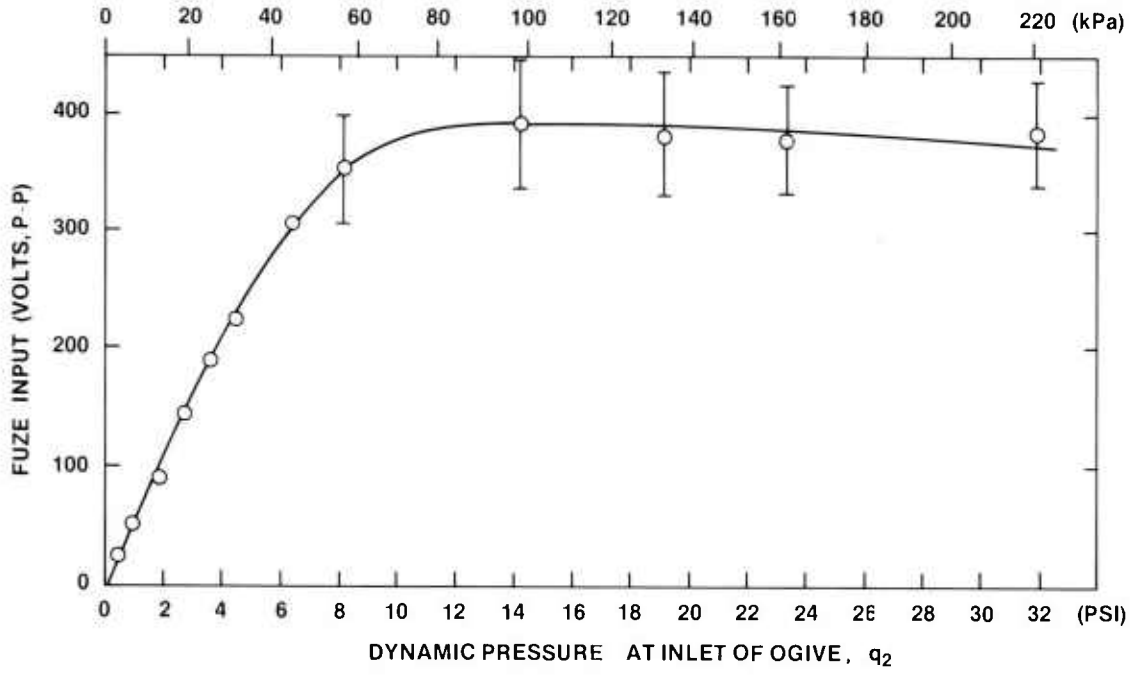

Figure 31. Laboratory calibration curve for high frequency fluidic generators used at Wallops Island, VA, field test.

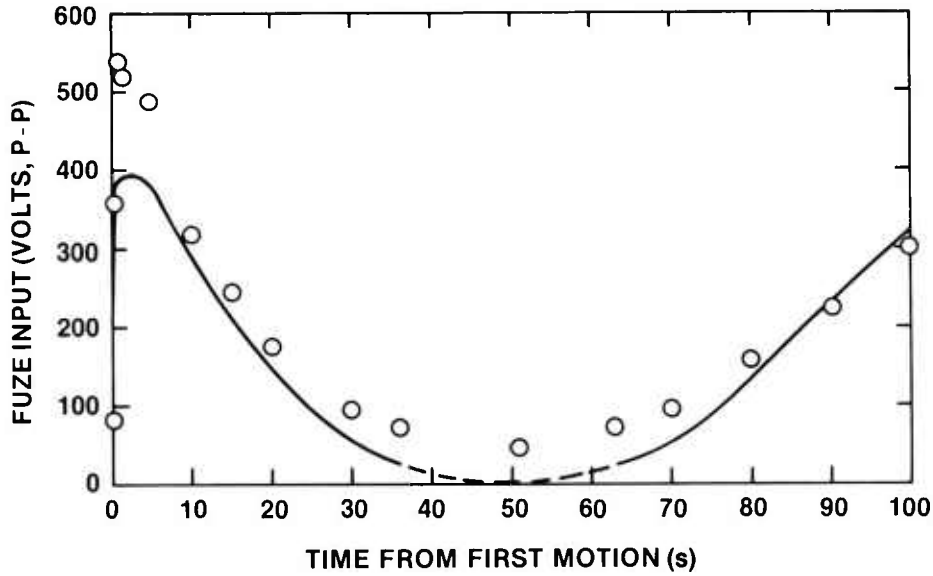

Figure 32. Expected (—) and measured (o) fuze input voltage during flight of ZAP rocket, round 9, at Wallops Island, VA, field test.

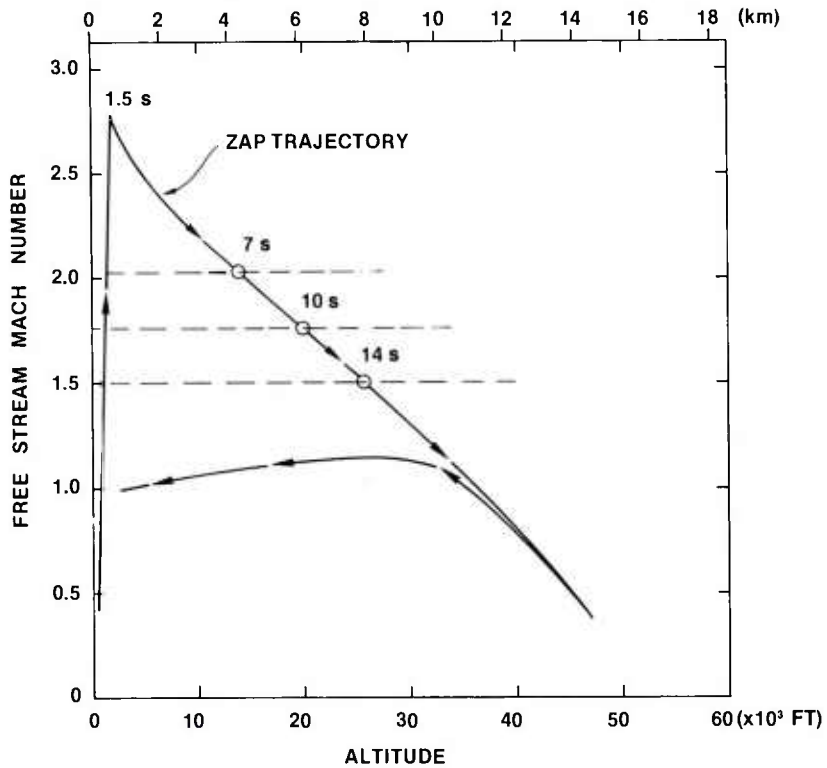

Figure 33. ZAP rocket trajectory and wind tunnel conditions.

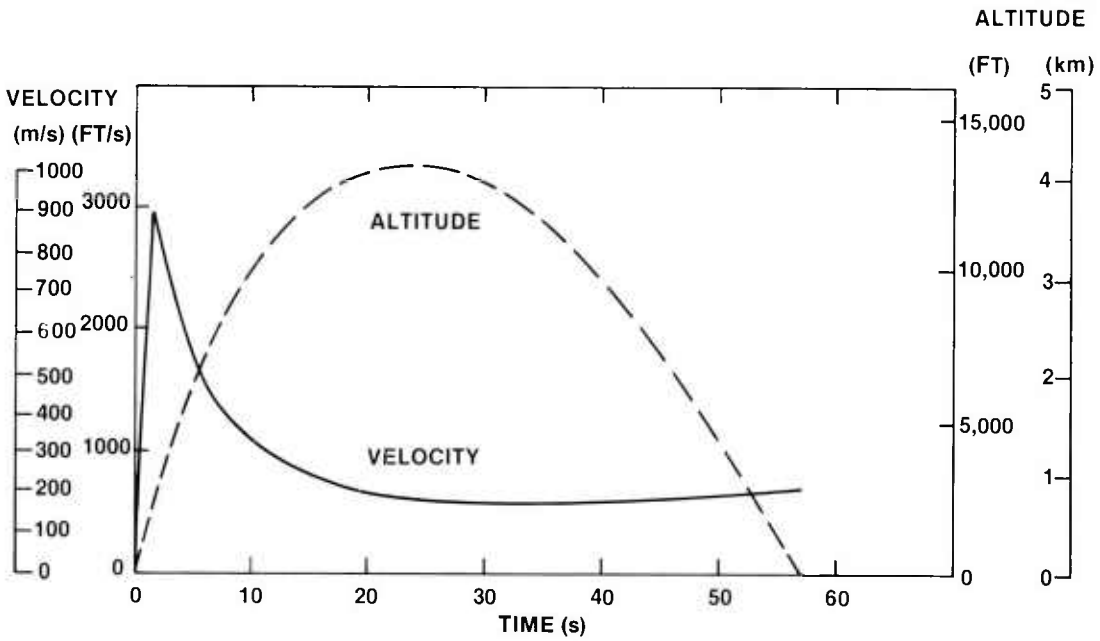

Figure 34. Trajectory of Zuni Mk 71 rocket, round 1, fuze 70, quadrant elevation = 42 deg, at Wallops Island, VA, field test.

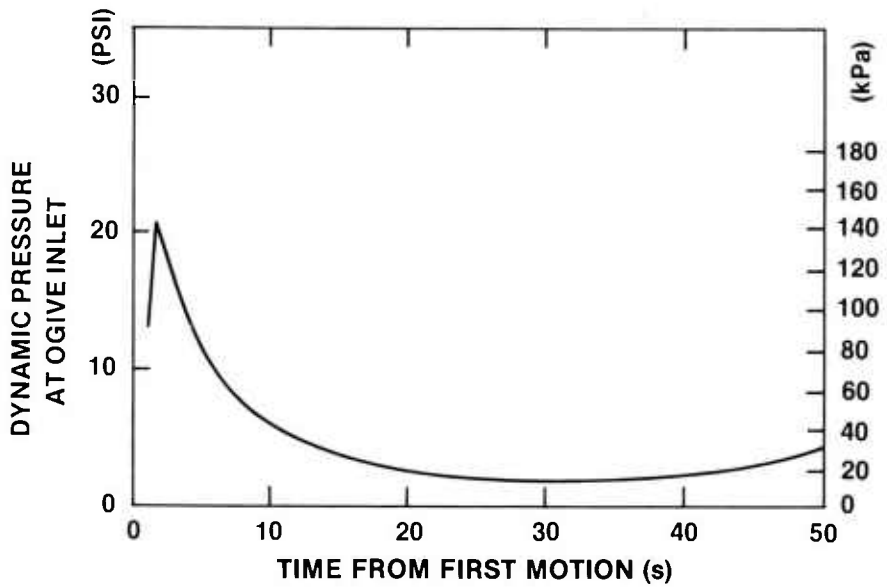

Figure 35. Variation of dynamic pressure at ogive inlet during flight of Zuni rocket, round 1, at Wallops Island, VA, field test.

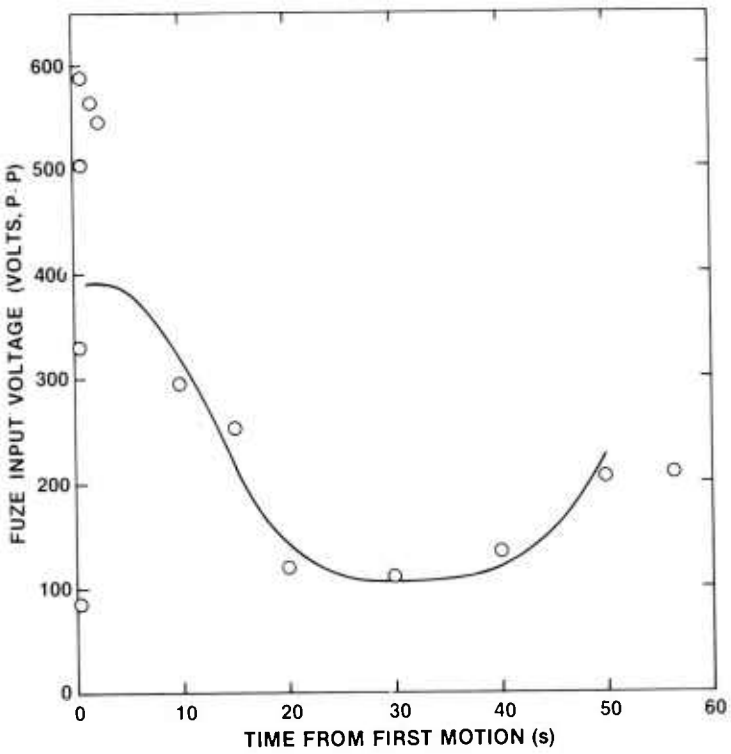

Figure 36. Expected (—) and measured (o) fuze input voltage during flight of Zuni rocket, round 1, at Wallops Island, VA, field test.

7.3 *Summary of Method Used to Predict Voltage Values in Wind Tunnel or in Field Tests*

A method was developed to relate wind tunnel, field test, and laboratory measurements. The method is based on the premise that the external flow parameter of dynamic pressure at the ogive inlet will produce the same values of voltage in the laboratory, in the wind tunnel, or in flight. This assumption is supported by the wind tunnel data of figures 23 and 24. The method will furnish a low estimate of voltage in the wind tunnel or in flight.

From laboratory measurements of voltage versus supply pressure for a given fluidic generator-fuze assembly, the values of q_2 may be calculated or read from the curve of figure 26. These values are plotted on a laboratory calibration curve of voltage versus q_2. Trajectory or wind tunnel conditions must be expressed in terms of Mach number and altitude. The values of q_2 can then be obtained from figure 25, in which q_2 is given as a function of Mach number and altitude.

By reversing the method, it is possible to determine the appropriate pressure in the laboratory to simulate a specified trajectory point. The Mach number and the altitude are obtained from trajectory data, and q_2 can then be found from figure 25. The required laboratory pressure is obtained from figure 26.

7.4 *Use of Method to Verify Operation of Improved Fluidic Generator in Wind Tunnel*

Since the data presented in the body of this report had been gathered, the fluidic generator was modified better to withstand the high pressures that occur at rocket burnout. This included an increase in reed thickness 0.457×10^{-3} m (0.018 in.) to 0.61×10^{-3} m (0.024 in.). This configuration, which is representative of the delivered power supplies, was tested recently at the National Aeronautics and Space Administration (NASA) Ames wind tunnel facility by Richard Goodyear of the Harry Diamond Laboratories.

A fuze was provided as an electrical load for the fluidic generator power supply. Although the fuze did not operate properly, as evidenced by output voltages that were monitored during the test, it appears from the excellent agreement between expected and measured voltage at the input to the fuze that the electrical load on the fluidic generator was not affected.

The voltage input to the fuze was measured in the laboratory and in the wind tunnel. The laboratory data are tabulated in table 5. The corresponding values of q_2 are calculated as described previously. Figure 37 shows the laboratory calibration curve of fuze input voltage versus q_2.

The wind tunnel conditions and measured fuze input voltage values are tabulated in table 6. The values of q_2 were calculated from the given tunnel conditions. The expected voltage values were obtained from table 6 for comparison with the measured values. The measured data were within 5 to 10 percent of the expected values over the Mach number range from Mach 0.4 to Mach 1.4. At Mach 0.3 (run 10), the discrepancy was higher, 20 percent. The altitude range for the supersonic Mach numbers was from 1.3 to 11.3 km (4400 to 37,200 ft). Thus, the method of relating laboratory measurements to wind tunnel conditions appears valid for the improved fluidic generator with the fuze as the electrical load.

TABLE 5. LABORATORY CALIBRATION DATA FOR FLUIDIC GENERATOR 201 WITH FUZE 221 AS ELECTRICAL LOAD

Pressure difference from inlet to exhaust ports		Calculated dynamic pressure at ogive inlet		Base voltage, Vb (V)	Fuze input = 2 × Vb (V p-p)
(kPa)	(psig)	(kPa)	(psig)		
6.89	1	6.68	0.97	25	50
13.78	2	12.96	1.88	48	96
20.6	3	19.3	2.80	70	140
27.5	4	25.16	3.65	90	180
34.4	5	30.88	4.48	105	210
48.2	7	41.71	6.05	125	250
62.0	9	51.98	7.54	150	300
103.4	15	72.25	10.48	190	380

Note: Pressure =101.35 kPa = 14.7 psia.

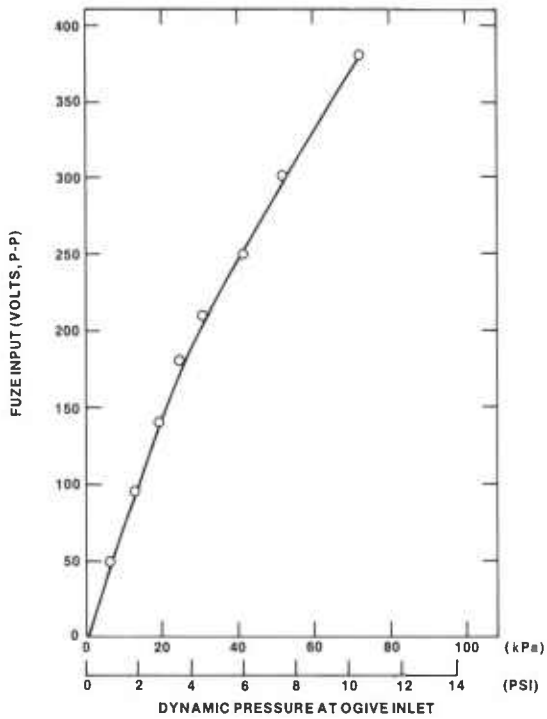

Figure 37. Laboratory calibration curve for fluidic generator 201 with fuze 221 as electrical load.

TABLE 6. FLUIDIC GENERATOR 201 OUTPUT IN NASA AMES WIND TUNNEL

Run	Mach No.	Altitude		Free stream total pressure		Dynamic pressure at ogive inlet		Fuze input	
		(km)	(ft)	(kPa)	(psia)	(k Pa)	(psia)	Measured (Vp-p)	Expected (Vp-p)
10	0.3	—	—	153.68	22.29	9.08	1.317	56	67
11	0.6	0.914	3,000	116.1	16.84	22.89	3.32	172	162
12	0.8	3.657	12,000	98.52	14.29	28.95	4.20	196	195
13	1.2	9.662	31,700	67.36	9.77	20.82	3.02	140	149
14	1.4	11.338	37,200	69.08	10.02	17.58	2.55	140	126
28	0.4	0.365	1,200	109.00	15.81	10.89	1.58	80	82
31	0.6	0.457	1,500	123.20	17.87	24.33	3.53	180	169
32	0.945	1.036	3,400	160.09	23.22	56.26	8.16	306	314
33	1.11	1.341	4,400	187.88	27.25	63.20	9 117	360	342
38	1.2	1.402	4,600	208.8	30.29	26.74	3.878	342	350
39	1.395	4.328	14,200	187.19	27.15	48.00	6.962	312	280

8. SUMMARY

A ram air driven power supply for the proposed MLRS high altitude rocket was tested in the NSWC supersonic wind tunnel. The test was similar to a previous test in November 1977, in which a resistance and a capacitance load were used on the power supply to simulate the fuze circuit. This test used a fuze as the electrical load.

The fluidic generator powered the fuze over the apex of a high altitude trajectory that represented low pneumatic energy input to the power supply. The voltage obtained at apex was only slightly above the required voltage to operate the fuze.

Tunnel data on both the fluidic generator and an alternator power supply up to altitudes of 21.33 km showed that the output of either type of power supply is independent of Mach number when the voltage is plotted versus dynamic pressure at the ogive inlet. A method was found to obtain values of q_2 for the laboratory or along flight trajectories. Several working curves were then developed to relate q_2 to laboratory measurements and to wind tunnel and flight conditions. Thus, expected voltage values in the wind tunnel or in flight were obtained from laboratory measurements of voltage versus pressure in an experimental arrangement as shown in figure 5. The method furnished a low estimate of voltage in the wind tunnel and in a recent field test of a fluidic generator and fuze fired on Zuni and ZAP rockets at high altitude.

ACKNOWLEDGEMENTS

The author acknowledges the assistance and the contributions of the following people at HDL: Henry Lee and Michael Salyards, who provided the power supplies and laboratory calibration data; LeRoy Hughes, Jerome Cooperman, and Dave Morrow, who assisted in gathering and reducing the wind tunnel data; Don Robinson, whose astute operation of the HDL data tape recorder contributed immensely to the success of the test and allowed it to take place as scheduled, despite the breakdown in the wind tunnel computer; Carl Campagnuolo, for his guidance in developing the theoretical model; and Richard Goodyear, for his contribution in the flight data analysis and use of results from the GSRS-6 Field Test Report.

The cooperation of the NSWC wind tunnel staff, especially Joe Knott, Steve Cothran, and Jay Marshall, in accomplishing test objectives is further appreciated.

DISTRIBUTION

ADMINISTRATOR
DEFENSE TECHNICAL INFORMATION CENTER
CAMERON STATION, BLDG 5
ATTN DTIC-DDA (12 COPIES)
ALEXANDRIA, VA 22314

COMMANDER
US ARMY RSCH & STD GP (EUP)
BOX 65
ATTN CHIEF, PHYSICS & MATH BRANCH
FPO NEW YORK 09510

COMMANDER
US ARMY ARMAMENT MATERIEL
READINESS COMMAND
ATTN DRSAR-LEP-L, TECHNICAL LIBRARY
ATTN DRSAR-ASF, FUZE & MUNITIONS
SUPPORT DIVISION
ROCK ISLAND, IL 61299

COMMANDER
US ARMY MISSILE & MUNITIONS
CENTER & SCHOOL
ATTN ATSK-CTD-F
REDSTONE ARSENAL, AL 35809

DIRECTOR
US ARMY MATERIEL SYSTEMS
ANALYSIS ACTIVITY
ATTN DRXSY-MP
ABERDEEN PROVING GROUND, MD 21005

DIRECTOR
US ARMY BALLISTIC RESEARCH LABORATORY
ATTN DRDAR-TSB-S (STINFO)
ABERDEEN PROVING GROUND, MD 21005

TELEDYNE BROWN ENGINEERING
CUMMINGS RESEARCH PARK
ATTN DR. MELVIN L. PRICE, MS-44
HUNTSVILLE, AL 35807

HQ USAF/SAMI
WASHINGTON, DC 20330

US ARMY ELECTRONICS TECHNOLOGY
AND DEVICES LABORATORY
ATTN DELET-DD
FORT MONMOUTH, NJ 07703

COMMANDER
US ARMY MISSILE COMMAND
ATTN DRCPM-RS
ATTN DRCPM-RSE, B. CROSSWHITE
ATTN DRCPM-RSE, B. RICHARDSON
REDSTONE ARSENAL, AL 35809

COMMANDER
NAVAL SURFACE WEAPONS CENTER
ATTN WX-40, TECHNICAL LIB
ATTN K81, J. HOLMES
ATTN K81, J. KNOTT
WHITE OAK, MD 20910

US ARMY ELECTRONICS RESEARCH
& DEVELOPMENT COMMAND
ATTN TECHNICAL DIRECTOR, DRDEL-CT

HARRY DIAMOND LABORATORIES
ATTN CO/TD/TSO/DIVISION DIRECTORS
ATTN RECORD COPY, 81200
ATTN HDL LIBRARY, 81100 (3 COPIES)
ATTN HDL LIBRARY, 81100 (WOODBRIDGE)
ATTN TECHNICAL REPORTS BRANCH, 81300
ATTN CHAIRMAN, EDITORIAL COMMITTEE
ATTN LEGAL OFFICE, 97000
ATTN CHIEF, BR 34400
ATTN CHIEF, BR 34200
ATTN CHIEF, BR 34600
ATTN CHIEF, BR 13400
ATTN CHIEF, BR 47400
ATTN BEARD, J., 34200
ATTN CROARKIN, J., 34400
ATTN FINGER, D., 34400
ATTN MORROW, D., 34400
ATTN CAMPAGNUOLO, C., 34600
ATTN DAVIS, H., 34600
ATTN GEHMAN, S., 13400
ATTN LEE, H., 34600
ATTN SALYARDS, M., 34600
ATTN GOODYEAR, R., 34600
ATTN GOTO, J., 13400
ATTN DEADWYLER, R., 13400
ATTN McCARL, W., 47400
ATTN TOKARCIK, J., 47100
ATTN FINE, J., 34600 (20 COPIES)
ATTN COOPERMAN, J., 34400